CHAPTER-3(A)

Synthesis, structures and Hirshfeld surface analysis of Ni(II) and Co(III) complexes with N_2O donor Schiff base ligand.

Abstract

Two octahedral complexes $[Ni(L2)(HL2)]ClO_4.0.5CH_3OH$ and $[Co(L2)_2]ClO_4$ have been synthesized with N_2O donor Schiff base ligand {((2-(phenyl amino)ethyl)imino)methyl}phenol (HL2) and characterized by spectroscopic techniques and single crystal X-ray diffraction studies. The molar conductivities data of the two complexes show that the complexes are 1:1 electrolyte. Single crystal X-ray diffraction data shows both Ni(II) and Co(III) complexes have distorted octahedral geometry and two ligands are coordinated to the metal centres and one ClO_4^- ion outside the coordination sphere. The intermolecular interactions in the complexes are evaluated by Hirshfeld surface analysis and revealed a significant contribution of non- or weakly polar interactions to the packing forces for both molecules, with crystal structure of **2** featuring short H/H contacts. Antimicrobial activity of the two complexes were studied by agar well diffusion method against Gram positive (*Bacillus subtilis*, *Streptococcus aureus*) and Gram negative (*Escherichia Coli*, *Proteus Vulgaris*) bacterial strains showed the complete inhibition of the tested strains by the complexes.

3(A).1. Introduction

Synthesis and characterization of transition metal complexes with Schiff base ligands have been an attractive area of research in coordination chemistry since long time because Schiff bases are versatile chelating ligand and the imine nitrogen and other donor atoms have important roles in coordination chemistry as they form stable complexes with different metal ions. The transition metal complexes with Schiff base ligand have wide applications in various fields of chemical sciences. Metal complexes with bi- and tridentate Schiff bases containing N and O donor atoms derived from aromatic amine and salicyldehyde have been studied extensively and there are many compounds reported in the literature [1-18].

During the search of literature, it is observed that there are many reports on complexes with the N_2O donor tridentate Schiff bases synthesized using salicyldehyde and its derivative with N-phenylethylenediamine [19-21]. The search in the Cambridge Crystallographic Database revealed the report of Al(III), Zn(II), Cu(II) and Mn(III) complexes with the N_2O donor Schiff base ligand{((2-(phenylamino)ethyl)imino) methyl}phenol (HL2) but there is no report on Ni(II) and Co(III) complexes with the ligand (HL2) to the best of our knowledge [22-25].

In this chapter, we describe the synthesis, characterization with structures of Ni(II) and Co(III) complexes with the Schiff base ligand {((2-(phenylamino)ethyl)imino)methyl}phenol (HL2). Structural data shows both Ni(II) and Co(III) complexes have slightly distorted octahedral geometry. The intermolecular interactions in the complexes are evaluated by Hirshfeld surface analysis. The antimicrobial activity of cobalt and nickel complexes against Gram Positive and Gram-negative bacterial strains has been discussed in details.

3(A).2. Experimental

3(A).2.1. Materials

The chemicals and solvents were of analytical grade and purchased from commercial sources. Salicyldehyde (Spectrochem), N-phenylethylenediamine (Aldrich) were used as received. $M(ClO_4)_2.6H_2O$ [M = Ni(II) and Co(II)] was prepared by reaction of metal carbonate with dilute $HClO_4$ acid and followed by slow evaporation of the solution over steam bath.

3(A).2.2. Synthesis of Ligand (HL2)

Ligand {((2-(phenylamino)ethyl)imino)methyl}phenol (HL2) was synthesized by literature method [23].

Yield: 1.70 g (92%). IR (KBr pellet) ν/ cm^{-1}; ν(N-H), 3200m; ν(C=N), 1604s; ν(O-H) 3386s. ^1H NMR (400 MHz, $CDCl_3$, δ/ppm): 3.51(2H, t, N-CH_2), 3.82(2H, q, N-CH_2), 6.628-8.32 (10H, m, aromatic protons and imine proton), 13.229 (1H, s, O-H), λmax/nm (εmax/mol^{-1} cm^{-1}). 309(173), 252(638).

Caution! Transition metal complexes with perchlorate ion and organic ligands are potentially explosive. Complexes should be synthesized in small quantities and handled with care

.

3(A).2.3. Syntheses of Complexes

3(A).2.3.1. Synthesis of $[Ni(L2)(HL2)]ClO_4.0.5CH_3OH$ (1)

A solution of ligand HL2 (0.120g, 0.5 mmol) in methanol was added drop by drop into a solution of nickel perchlorate hexahydrate (0.091g, 0.25mmol) in methanol (10ml) at room temperature and colour changed to dark green immediately. Stirring was continued for 2 hr, filtered and solution was kept for evaporation at room temperature. Green hexagonal plate crystals suitable for single crystal X-ray diffraction were obtained from the mother liquor after several days.

Yield 0.098g (65%). Found C = 48.35, H = 4.38, N = 8.40%, Elemental analysis calc. for $C_{31}H_{34}N_4O_7ClNi$: C = 48.45, H = 4.42, N = 8.38%. IR (KBr pellet)/ cm^{-1}; ν(N-H), 3295 m; ν(C=N), 1600 s; ν(M-O), 567 s; ν(M-N), 481s; ν(ClO_4), 1106s; δ(O-Cl-O), 622m. λ_{max}/nm (ε_{max} /mol^{-1} cm^{-1}). 885(43), 583(20), 379(147), 310(159), 247(1188). Λ_M ($\Omega^{-1}cm^2$ mol^{-1}) = 120. μ_{eff} = 2.81 BM.

3(A).2.3.2. Synthesis of $[Co(L2)_2]ClO_4$ (2)

The complex was synthesized by using same method as that of complex **1** except cobalt perchlorate hexahydrate was used instead of nickel perchlorate hexahydrate. Red-brown square plate type crystals suitable for single crystal X-ray diffraction were obtained from the mother liquor after several days.

Yield. 0.113g (75%). Found C = 56.28, H = 4.60, N = 8.67 %, Elemental analysis calc. for $C_{30}H_{30}N_4O_6ClCo$: C = 56.56, H = 4.71, N = 8.80%. IR (KBr pellet)/ cm^{-1}; ν(N-H), 3217 m; ν(C=N), 1599 s; ν(M-O), 554 s; ν(M-N), 465 s; ν(ClO_4), 1077 s; δ(O-Cl-O), 685s. λ_{max}/nm (ε_{max}/$mol^{-1}cm^{-1}$). 718(11), 504(41), 393(155), 299(811), 240(1243). ^1H NMR: (500 MHz, $CDCl_3$, δ/ppm): 6.38 – 7.64 (m, 10H, aromatic ring proton and imine proton), 4.18 (dd, 2H, J = 10 Hz, N-CH_2), 2.95 (d, 2H, J = 10 Hz, N-CH_2). Λ_M ($\Omega^{-1}cm^2$ mol^{-1}) = 118.

3(A).2.4. Physical Measurements

The IR spectra were recorded on Bruker alpha FT-IR spectrometer using KBr pellet. UV-Vis spectra were recorded on a JASCO V- 630 spectrophotometer in acetonitrile solution. ^{1}H NMR spectra were recorded on Bruker NMR AV400 and Bruker, Avance II (500MHz) spectrometers in $CDCl_3$. The elemental analysis (C, H and N) were carried out using a Thermo Finnigan FLASH EA 1112 series elemental analyser. Solution conductivity were measured in acetonitrile solution using Equip-Tronics conductivity meter (model no. EQ660 A). Room temperature magnetic susceptibilities of powder samples were measured using Guoy balance.

3(A).2.5. Antimicrobial activity assay

The antimicrobial activity of the compounds was tested against Gram positive (*Bacillus subtilis*, *Streptococcus aureus*) and Gram negative (*Escherichia Coli*, *Proteus Vulgaris*) bacterial strains by agar well diffusion method assay. Various concentrations of the ligand and the complexes were prepared in DMSO. The overnight grown bacterial cultures were spread on 4 mm thick Luria Bertani (LB) agar plates. DMSO and 1 mg/mL of chloramphenicol were used as a negative control and positive control respectively. The test samples or the controls were added to the wells (5 mm diameter) made in the agar plates. The assay was performed in duplicates. The plates were then incubated at 37˚C for 24 h. The plates were checked for appearance of zones of inhibition after incubation. The lowest concentration of the test sample which prevented visible growth of microorganism, which thus resulted in the formation of zone was considered as MIC of that sample

3(A).3. X-ray Crystallography

The X-ray single crystal data of the complexes **1** and **2** were collected on an Agilent Technologies Xcalibur diffractometer with CCD area detector, equipped with graphite monochromated Mo Kα radiation (λ = 0.71073 Å) at 273K. The 2θ range for data collection was from 6.192^0 to 50^0 for complex **1** and 6.76^0 to 58.36^0 for complex **2**.

Table 3(A).1 Crystallographic data for Ni(II) and Co(III) Complexes.

	[Ni(HL2)(L2)]ClO_4.0.5CH_3OH	**[$Co(L2)_2$].ClO_4**
Empirical formula	$C_{61}H_{62}Cl_2N_8Ni_2O_{13}$	$C_{30}H_{30}ClCoN_4O_6$
Formula weight	1303.50	636.96
Temperature/K	293(2)	295
Crystal system	Monoclinic	Orthorhombic
Space group	$P2_1/c$	$C222_1$
a/Å	20.5999(8)	9.5746(10)
b/Å	13.8559(5)	15.0919(16)
c/Å	21.8999(8)	20.051(3)
α/°	90	90
β/°	106.166(4)	90
γ/°	90	90
Volume/$Å^3$	6003.7(4)	2897.3(6)
Z	4	4
ρ_{calc} g/cm^3	1.442	1.460
μ/mm^{-1}	0.787	0.735
F(000)	2712.0	1320.0
Crystal size/mm^3	0.41 × 0.21 × 0.20	0.22 × 0.18 × 0.15
Radiation	MoKα (λ = 0.71073)	MoKα (λ = 0.71073)
2θ range for data collection/°	6.192 to 50	6.758 to 58.37
Index ranges	-24 ≤ h ≤ 24 -16 ≤ k ≤ 16 -26 ≤ l ≤ 26	-12 ≤ h ≤ 13, -19 ≤ k ≤ 20, -24 ≤ l ≤ 25
Reflections collected	56897	9162
Independent reflections	10554 [R_{int} = 0.0637, R_{sigma} = 0.0491]	3423 [R_{int} = 0.0592, R_{sigma} = 0.0901]
Data/restraints/ Parameters	10554/0/777	3423/0/191
Goodness-of-fit on F^2	1.018	1.026

Final R indexes [I>=2σ (I)]	R_1 = 0.0548, wR_2 = 0.1370	R_1 = 0.0676, wR_2 = 0.1437
Final R indexes [all data]	R_1 = 0.0885, wR_2 = 0.1639	R_1 = 0.1254, wR_2 = 0.1808
Largest diff. peak/hole/e $Å^{-3}$	0.72/-0.53	0.69/-0.26
CCDC number	2011260	1960452

The data interpretations were processed with CrysAlisPro, Agilent Technologies, Version 1.171.35.19 [26] and an absorption correction based on multi-scan method was applied [27]. Both the structures were solved by direct methods and refined anisotropically by the full-matrix least-square based on F^2 technique using SHELXL-97 program package [28]. Hydrogen atoms were positioned geometrically and refined with a riding model. All calculations were performed using the SHELXTL97 package. The data collection and refinement parameters are summarized in Table 3(A).1.

3(A).4. Results and discussion

3(A).4.1. Syntheses

Mononuclear octahedral Ni(II) and Co(III) complexes have been synthesized with good yield (>65%) by the reaction of metal perchlorate hexahydrate and tridentate NNO donor Schiff base ligand HL2 in 1:2 mole ratio in methanol at room temperature [Scheme 3(A).1]. The cobalt complex is diamagnetic, confirming the change of oxidation state of cobalt(II) to cobalt(III) during synthesis and one perchlorate anion is outside the coordination sphere inorder to balance the charge of cobalt(III). The ligand is tridentate with N_2O coordination sites and form octahedral complexes with both Ni(II) and Co(III) but in the nickel(II) complex, two ligands are coordinated as L2 and HL2 and one ClO_4^- outside the coordination sphere.

Molar conductivity measurements in CH_3CN shows both the complexes are 1:1 electrolyte and this was confirmed by IR spectral data. The molecular composition of the complexes has been confirmed by elemental analyses and single crystal X-ray diffraction studies. The complexes are soluble in common organic solvents such as CH_3CN, alcohol, methylene chloride, acetone, chloroform etc.

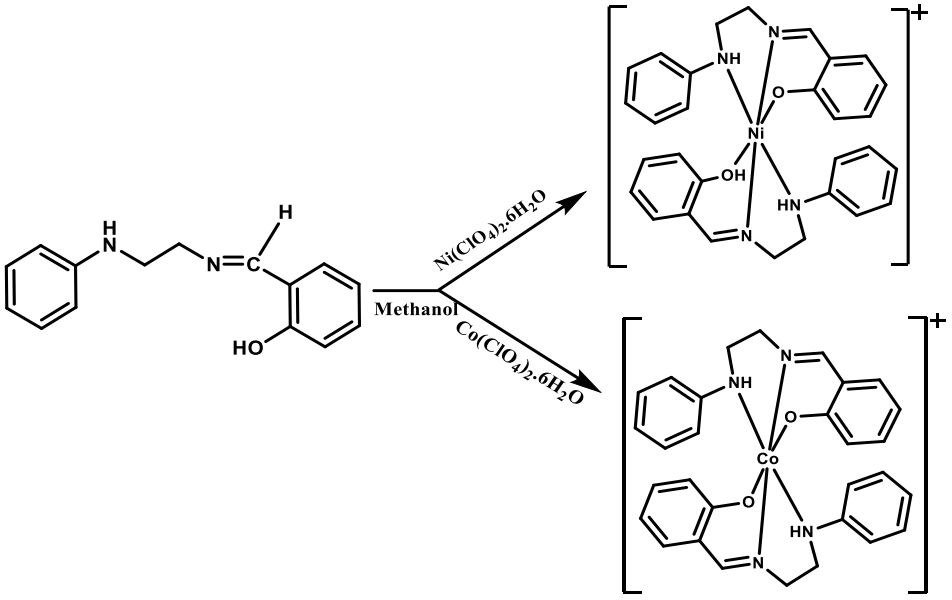

Scheme 3(A).1. Syntheses of the complexes

3(A).4.2. Spectral Data

3(A).4.2.1. ^{1}H NMR and Mass Spectral data.

The ^{1}H NMR spectrum of ligand (HL2) shows one triplets appeared in the region at 3.51 ppm and one quartered appeared in the region at 3.82 ppm confirming the presence of $–CH_2–CH_2–$ group of ethylenediamine moiety. One singlet appear at 13.229 ppm confirms the presence of OH group and another singlet appeared at 8.34 ppm confirming the presence of imine (HC=N) group. The aromatic protons of phenyl ring appeared as multiplet at 6.62-8.32 ppm.

The ^{1}H NMR data for the cobalt(III) complex recorded in $CDCl_3$ is presented in the experimental section. All the aromatic protons and imine proton of the coordinated Schiff base ligand appeared in the region of 6.38–7.64 ppm and protons appeared in the region of 2.87–4.40 ppm are assigned to $N–CH_2–CH_2–N$ protons. Coordination environment of cobalt(III) center is also confirmed by single crystal X-ray diffraction studies.

Mass spectrum of the synthesized Schiff base ligand (HL2) confirmed the proposed formula by detecting the following peaks. The observed peak at m/z 240 ($C_{15}H_{16}N_2O$), represent the molecular ion peak of the Schiff base with 100% abundance. The other molecule ion peaks (77,106,195) appeared in the mass spectrum are attributed to the fragmentation of molecule obtained from the rupture of different bonds inside the molecule. From the data we concluded

that the molecular weight was in good agreement with this of the calculated molecular weight of the investigated ligand HL2.

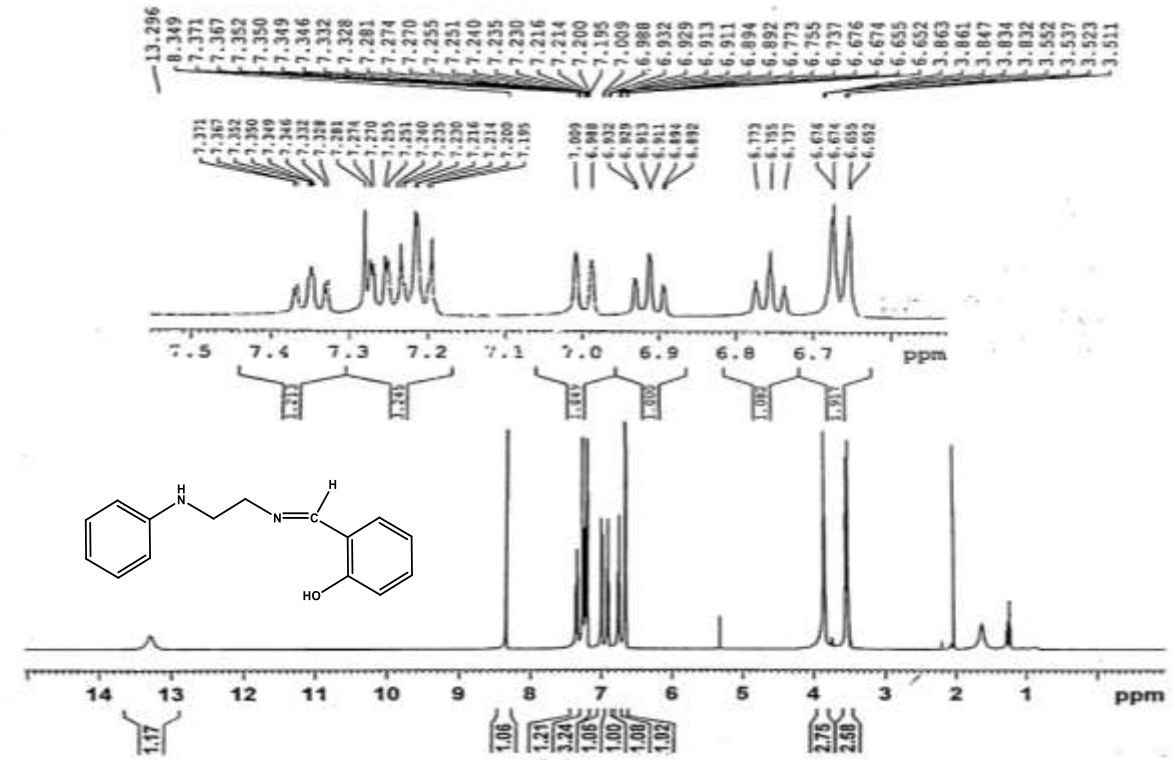

Figure.3(A).1. ^{1}H NMR Spectrum of Ligand (HL2)

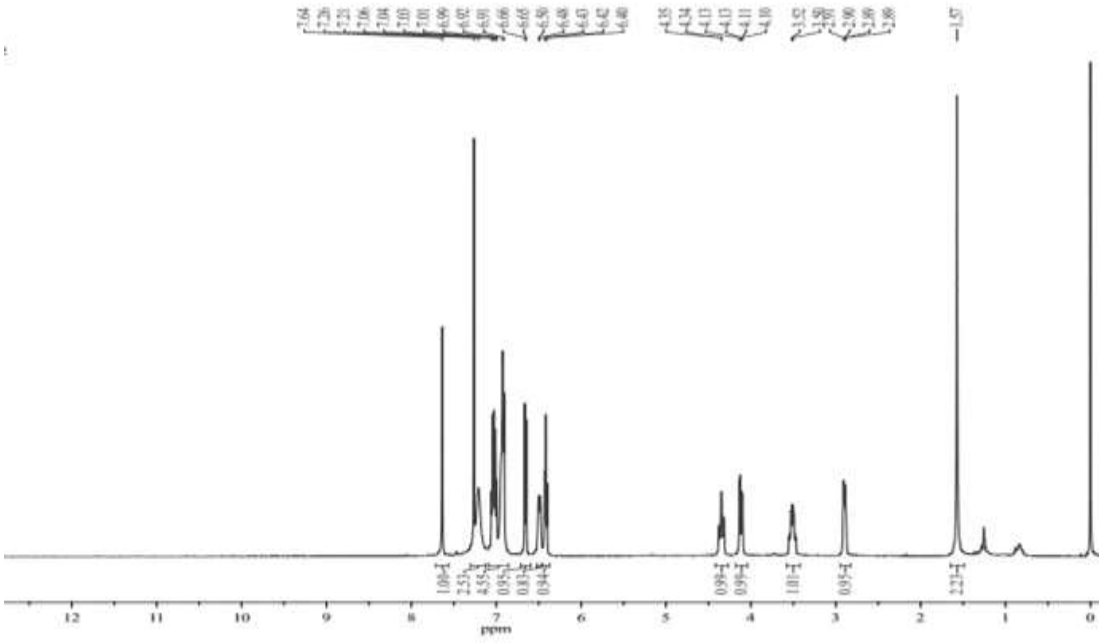

Figure.3(A).2. ^{1}H NMR Spectrum of $[Co(L2)_2]ClO_4$

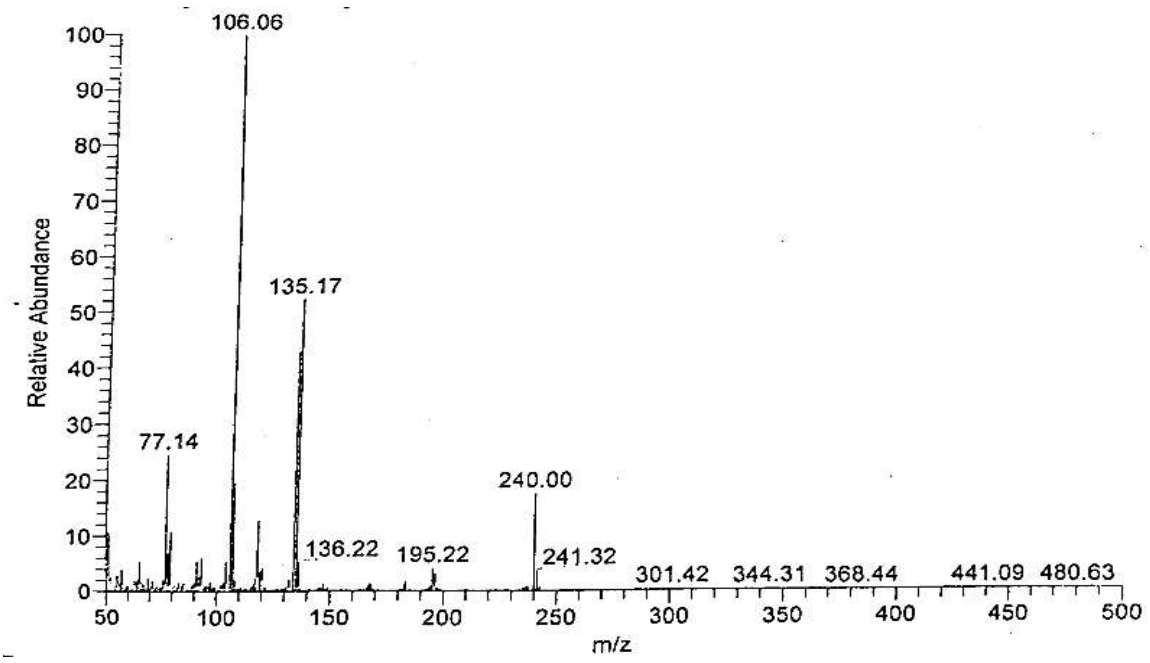

Figure.3(A).3. Mass Spectrum of ligand (HL2)

3(A).4.2.2. IR Spectral data

The IR spectrum of the complexes were assigned with respect to IR spectrum of the free ligand HL2 in order to determine the coordination of ligand to both the metal centres. The strong absorption band exhibited at ~1600 $cm^{-1}$of the complexes as well as ligand and the bands are shifted to lower wave numbers in the range of 5 cm^{-1} in the complexes in comparison to ligand which may be attributed to the coordination of the imine nitrogen atom to the nickel and cobalt centres in the complexes. One weak and broad absorption band ~ 3450 cm^{-1} for complex **1** is due to ν(O-H) stretching vibration of the methanol and this band is absent in the complex **2**. One weak but sharp band appeared at ~3250 cm^{-1} due to ν(NH) group for both the complexes. All the complexes exhibited bands at ~550 due to ν(M-O) and one strong band at ~465 cm^{-1} is due to υ(M-N). Both the complexes exhibited a strong absorption band at 1040 cm^{-1} and a weak band at ~640cm^{-1} due to δ(O-Cl-O) indicating non-coordinating ClO_4^- outside the coordination sphere [29].

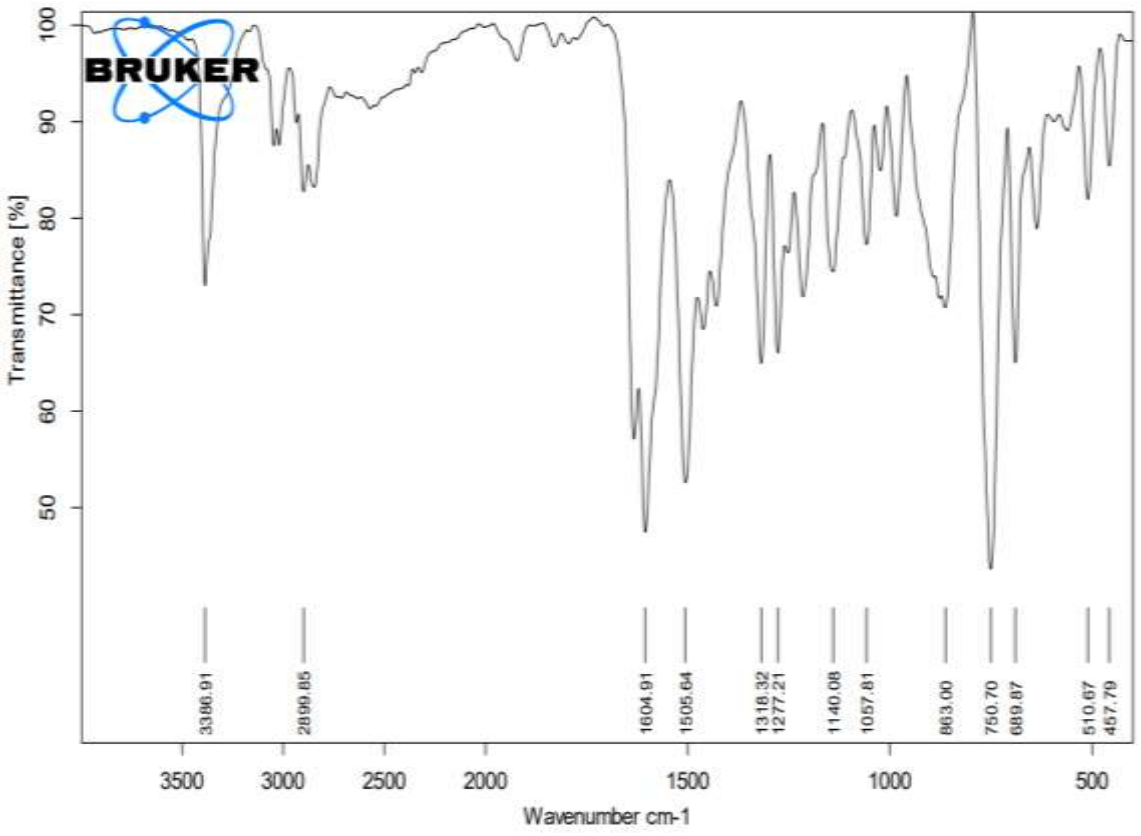

Figure. 3(A).4. IR spectrum of Ligand(HL2) **(1)**

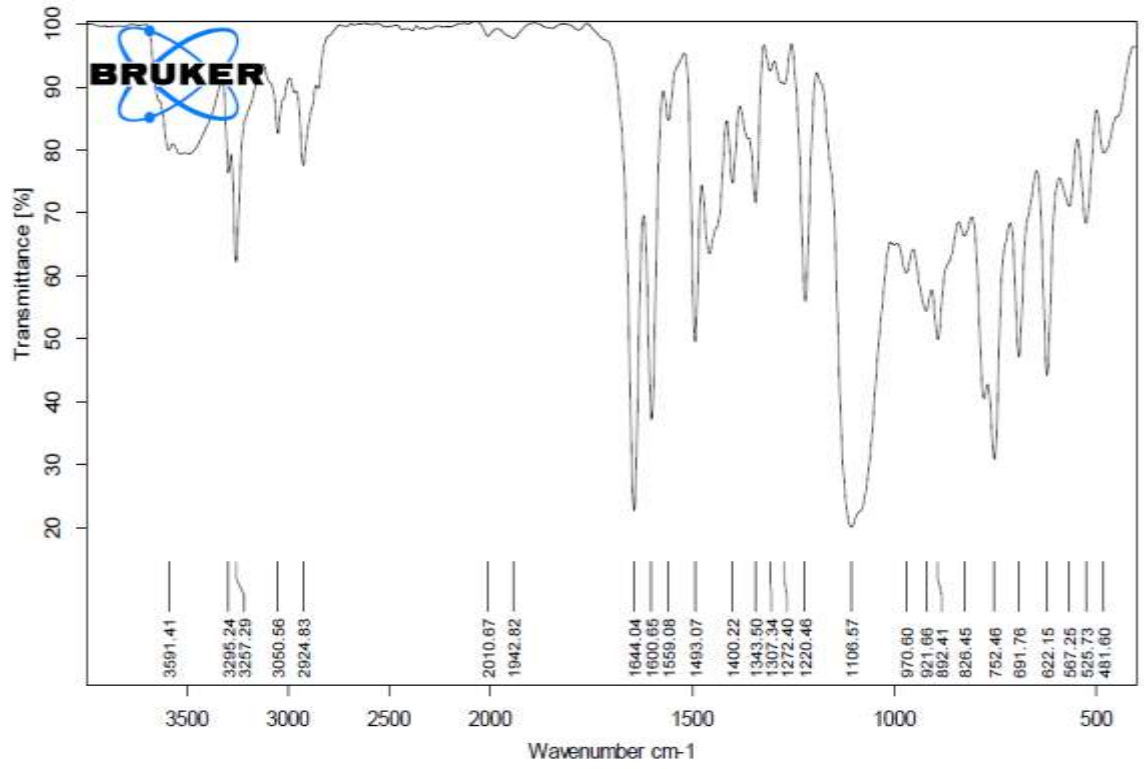

Figure. 3(A).5. IR spectrum of $[Ni(L2)(HL2)]ClO_4.0.5CH_3OH$ **(1)**

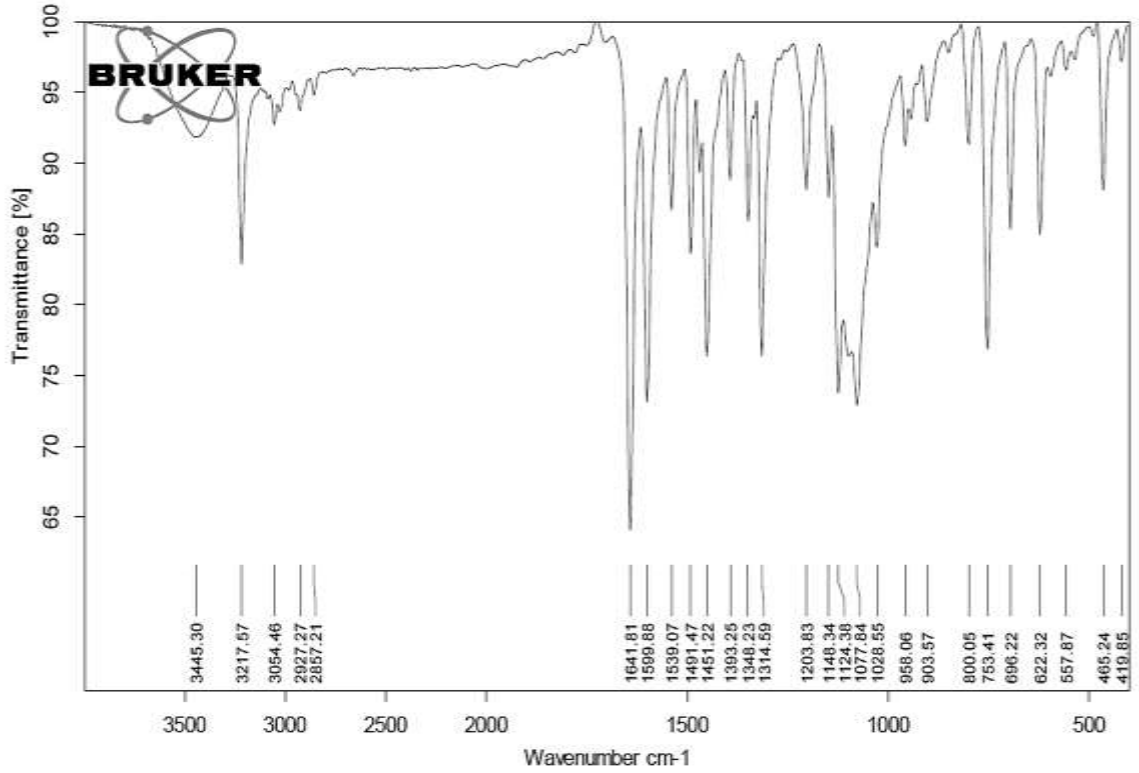

Figure. 3(A).6. IR spectrum of $[Co(L2)_2]ClO_4$ **(2)**.

3(A).4.2.3. Electronic spectral data

The electronic spectra of the complexes were drawn in CH_3CN solution at room temperature. The higher energy bands observed at less than 400 nm are due to charge transfer and intra ligand transition [8]. The nickel(II) complex exhibited one band at 885 nm with molar extinction coefficient 41 L mol^{-1} cm^{-1} which is due to d-d transition.

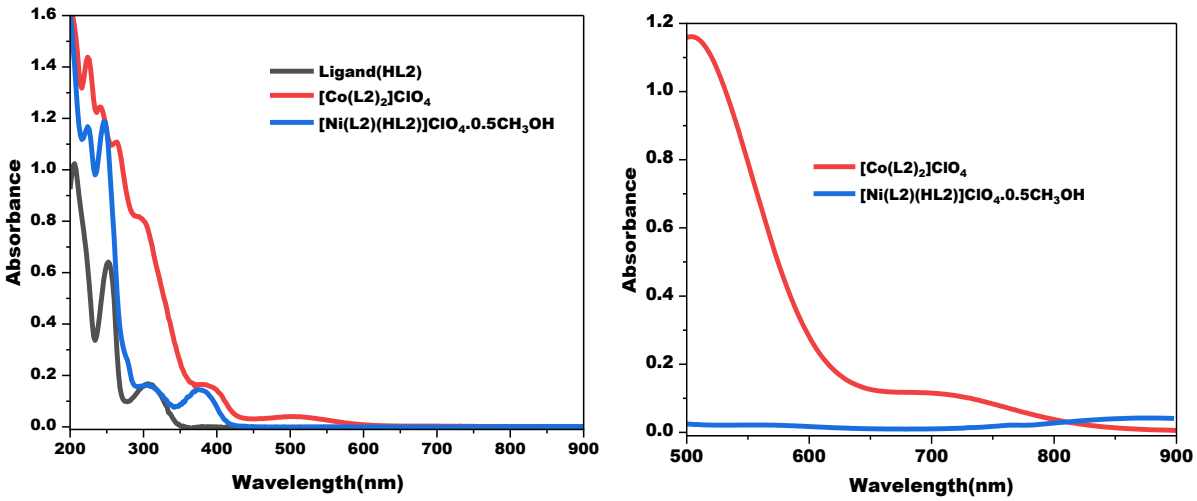

Figure. 3(A).7. Electronic spectra of the complexes in CH_3CN (10^{-3} M).

The cobalt(III) complex shows two absorptions bands- one band at 504 nm with molar extinction coefficient 41 L mol^{-1} cm^{-1} and another band at 718nm with 11 L mol^{-1} cm^{-1} due to d-d transition or ligand field transitions. [8,9].

3(A).4.2.4. Magnetic data

The magnetic susceptibility measurements in the powder samples show that the effective magnetic moment (μ_{eff}) of the nickel complex at room temperature is 2.80 B.M. indicating two electron paramagnetism but cobalt(III) complex is diamagnetic.

3(A).4.3. Structures of the complexes

3(A).4.3.1. Description of structure of $[Ni(L2)(HL2)]ClO_4.0.5CH_3OH$

The ORTEP diagram of the complex with atom-labelling scheme is shown in Fig.3(A).8 and selected bond lengths and angles are given in Table 3(A).2. The molecule crystallizes in monoclinic crystal system with space group $P2_1/c$.

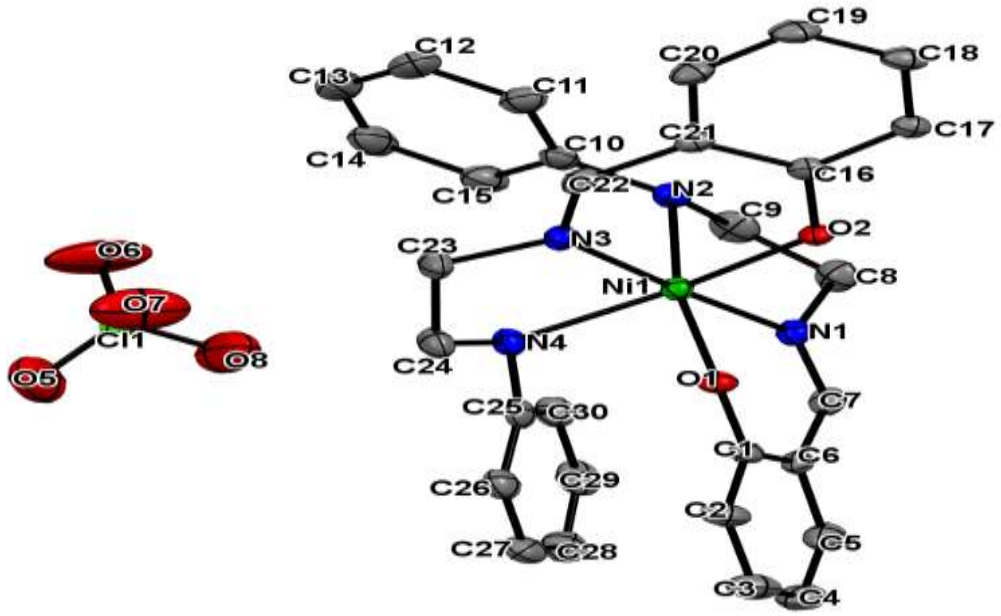

Figure.3(A).8. ORTEP diagram of the complex **1** with atom numbering scheme. Hydrogen atoms and CH_3OH molecule are omitted for clarity.

The structure determination confirmed that the complex **1** is ionic and each molecule has one ClO_4^- anion is outside the coordination sphere. There are two nickel centres, two ClO_4^- anions and one CH_3OH molecule in the asymmetric unit. In the structure, nickel(II) has six coordination using four nitrogen atoms N1, N2, N3, N4 and two oxygen atoms O1, O2 from

two tridentate ligands and two N_2O donor Schiff base ligands are coordinated as HL2 and L2. The equatorial positions of the octahedron are occupied by three nitrogen atoms N1, N2, N3 and oxygen atom O1 and the axial positions are occupied by one nitrogen atom N4 and one oxygen atom O2. The bond distance Ni-N2 (2.220 Å) is longer than the other three bond lengths Ni-N1(1.995), Ni-N3(2.000Å) and Ni-O1(2.086Å) in the equatorial plane. The distances in the axial planes Ni-N4(2.210 Å) and Ni-O2(2.081 Å) are not same and the axial bond angle N4-Ni1-O2 (169.00^0) is not linear. The geometry around the nickel (II) centre is distorted octahedral which can be described from unequal bond angles and bond lengths.

3(A).4.3.2. Description of structure of $[Co(L2)_2]ClO_4$

The ORTEP diagram of the complex with atom numbering scheme is shown in Fig 3(A).9. The molecule crystallizes in orthorhombic crystal system with space group *$C222_1$*.

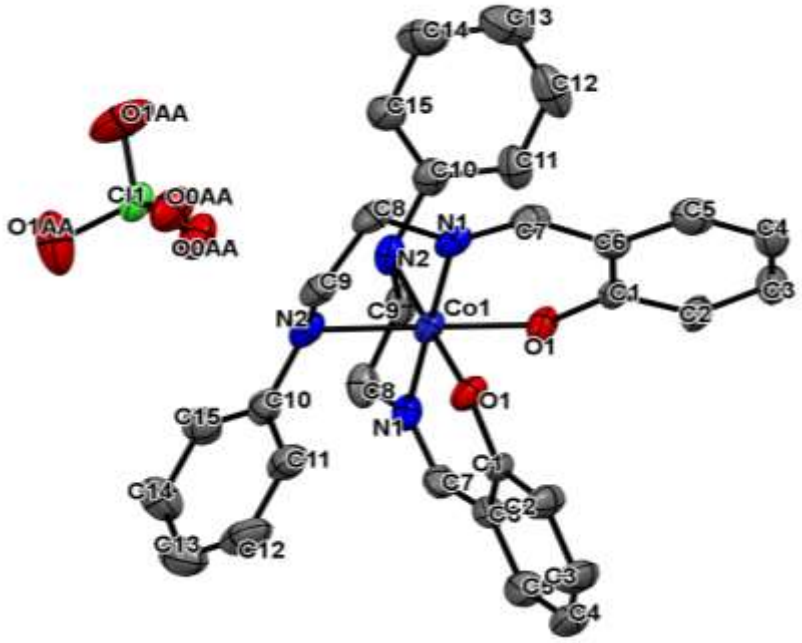

Figure.3(A).9. ORTEP diagram of the complex **2** with atom numbering scheme. Hydrogen atoms are omitted for clarity

The structure shows each cobalt centres has six coordination and two tridentate ligands are coordinated and one perchlorate anion is outside the coordination sphere. The bond distances in the horizontal as well as axial planes are in the range of 1.865 to 2.053Å and these are very close to each other. The axial bond angle N7-Ni-O3 is 177.70 which is nearly linear. The

geometry around the cobalt (III) centre is slightly distorted octahedral which are due to unequal bond angles and bond lengths.

Table 2(A).2 Selected bond lengths (Aº) and bond angles (º) for the complexes

$[Ni(HL2)(L2)]ClO_4.0.5CH_3OH$		**$[Co(L2)_2]ClO_4$**	
Bond lengths(Å)			
Ni1- N1	1.995(3)	Co1- O1	1.864(4)
Ni1- N3	2.000(3)	Co1- $O1^1$	1.864(4)
Ni1- O2	2.081(3)	Co1- $N1^1$	1.905(5)
Ni1- O1	2.086(3)	Co1- N1	1.905(5)
Ni1-N4	2.210(3)	Co1- $N2^1$	2.056(5)
Ni1-N2	2.220(4)	Co1- N2	2.056(5)
Bond angles (^{0})			
N1-Ni1-N3	175.77(15)	$O1^1$-Co1-O1	90.48(3)
N1-Ni1-O2	91.33(12)	$N1^1$-Co1-$O1^1$	93.73(19)
N3-Ni1-O1	97.90(13)	$N1^1$-Co1-O1	85.66(18)
O2-Ni1-O1	85.56(11)	N1-Co1-$N1^1$	179.13(3)
N3-Ni1-N4	81.71(14)	$N2^1$-Co1-O1	87.5117)
O2-Ni1-N4	169.00(13)	N2-Co1-O1	177.77(19)
O1-Ni1-N2	167.80(12)	$N2^1$-Co1-$N1^1$	85.13(2)
N1-Ni1- N2	82.37(14)	N2-Co-$N1^1$	95.44(2)
N1-Ni1-O1	86.22(13)	N2-Co-$N2^1$	94.52(3)

3(A).4.4. Molecular Hirshfeld Surface Analysis

Molecular Hirshfeld surface analysis was performed to gain insights regarding important intermolecular interactions present in the crystal. The calculation was performed using Crystal Explorer 17.5 [30] program. Hirshfeld surface analysis [31] is an effective tool for

understanding packing modes in molecular crystals as well as quantifying the intermolecular interactions. The d_{norm} are mapped over the 3D Hirshfeld surfaces using a red–blue–white color scheme. The normalized contact distance d_{norm} is related to *d*e (distance from the point to the nearest nucleus external to the surface), *d*i (distance to the nearest nucleus internal to the surface) and the van der Waals (vdW) radii of the atom. The red regions correspond to closer contacts with negative *d*norm value, the blue regions correspond to longer contacts with positive *d*norm value and the white regions are those where the distance of contacts is exactly the van der Waal's separation and with a *d*norm value of zero. Another two important colour coded properties e.g. shape index and curvedness which are based on the local curvature were also mapped. The shape index is extremely sensitive to the change in surface shape. The curvedness is a measure of the shape of the surface area of the molecule. All the generated surfaces are presented in transparent mode to facilitate better visualization. Further two dimensional (2D) fingerprint (FP) plot were mapped over the surface to highlight the nature of the intermolecular interactions. It summarizes all the intermolecular contacts experienced by the molecule quantitatively. The splitting of FP into specific atom...atom contacts in a crystal provides the contribution in percentage of different types of intermolecular contacts experienced by the molecule.

Molecular Hirshfield surfaces comprising of *d*norm surface, shape index and curvedness of the complex **1** and **2** were generated using a standard (high) surface resolution and is illustrated in [Fig. 3(A).10]. The *d*norm surface was mapped on over the range of -0.7752 to 1.8752 for complex **1** and from -0.4324 a.u. to +1.3900 a.u. for complex **2**,, shape index is in the range of -1.000 a.u. to 1.000 a.u. and curvature in the range of -4.000 a.u. to 0.4000 a.u. for both the complexes. The *d*norm mapping of complex **1** and **2** indicates strong O-H···O hydrogen bonding interaction as primary interaction seen as bright red spot. The two dimensional(2D) fingerprint plots from Hirshfeld surface analyses of complex **1** and **2** is shown in Fig.3(A).11

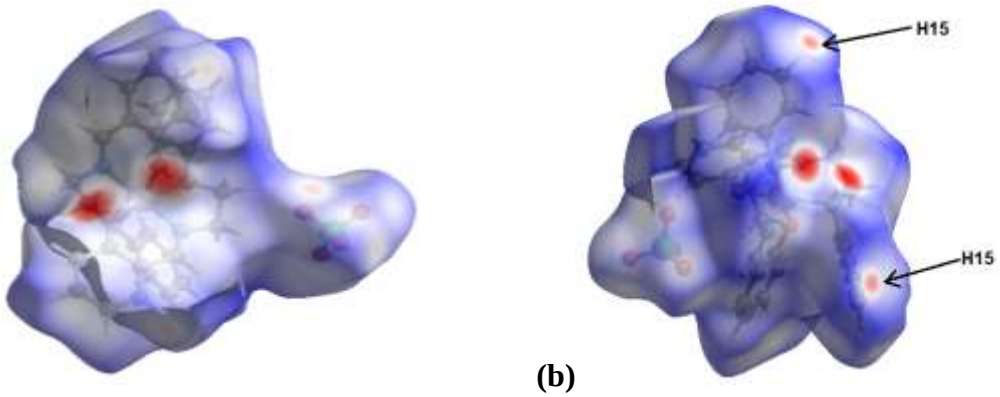

(a) **(b)**

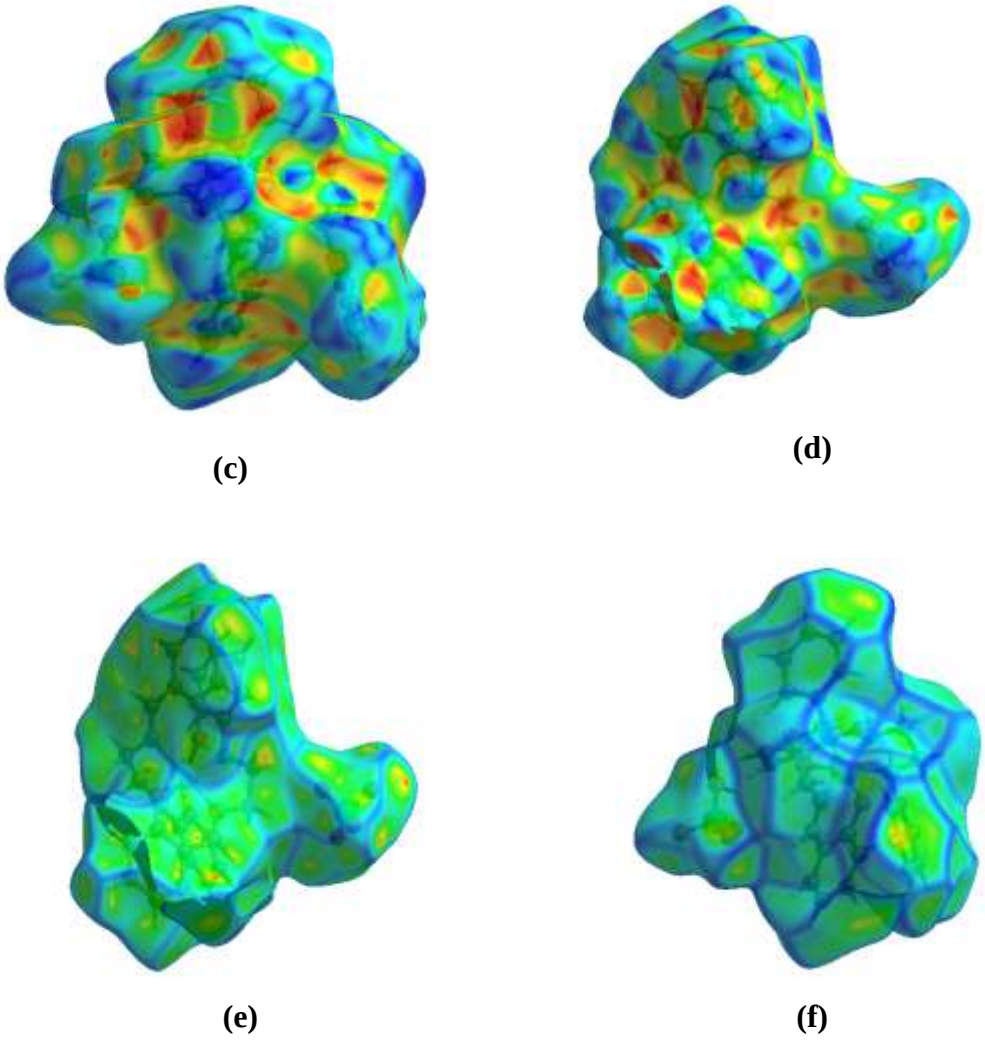

(c) **(d)**

(e) **(f)**

Fig.3(A).10. Hirshfeld surfaces mapped for *d*norm surfaces (a and b), shape index (c and d) and curvature (e and f) of complexes **1**and **2** respectively**.**

and [Fig. 3(A).12] respectively which illustrate the relative contribution (in percentage) of the major intermolecular contacts associated with it. The 2D Finger print plots complement the Hirshfeld surface by summarizing the nature and type of intermolecular contacts in a quantitative manner. The most important interaction is H···H (large spike) with contribution of 56.1% for complex **2** and 46.0% for complex **1** to the overall crystal packing. Complex **2** exhibits very short H···H contacts involving H15 of each phenyl ring of the HL ligand connected to a single N atom which is absent in complex **1**. Similar short H···H contacts are reported in 1-deoxy-1-(N-methylphenylamino)-D-psicose molecule reported by Mossine et al [32] and (4-nitrophenyl)methyl 2,3-dihydro-1H-pyrrole-1 carboxylate molecule reported by Tan et al.[33]. Existence of such short H···H contacts although are rare but possible in few crystals which can

be both attractive or repulsive. In case of complex **2,** the distortion is less compared to complex **1** and thus stability of the complex **2** may be higher because of this short H···H contacts.

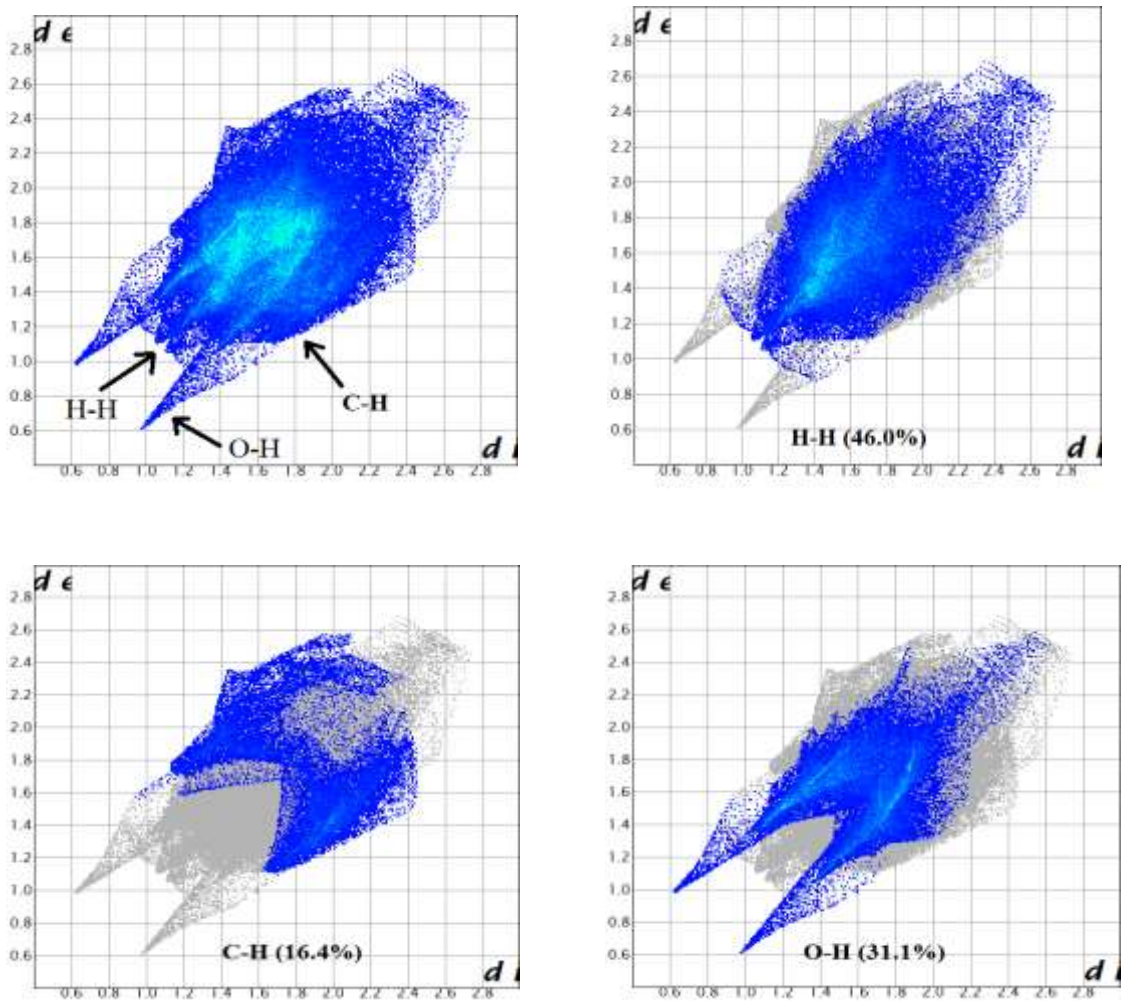

Fig.3(A).11. Fingerprint plot of **1**: full and resolved into H···H, C···H and O···H contacts showing the percentages of contacts contributed to the total Hirshfeld surface area.

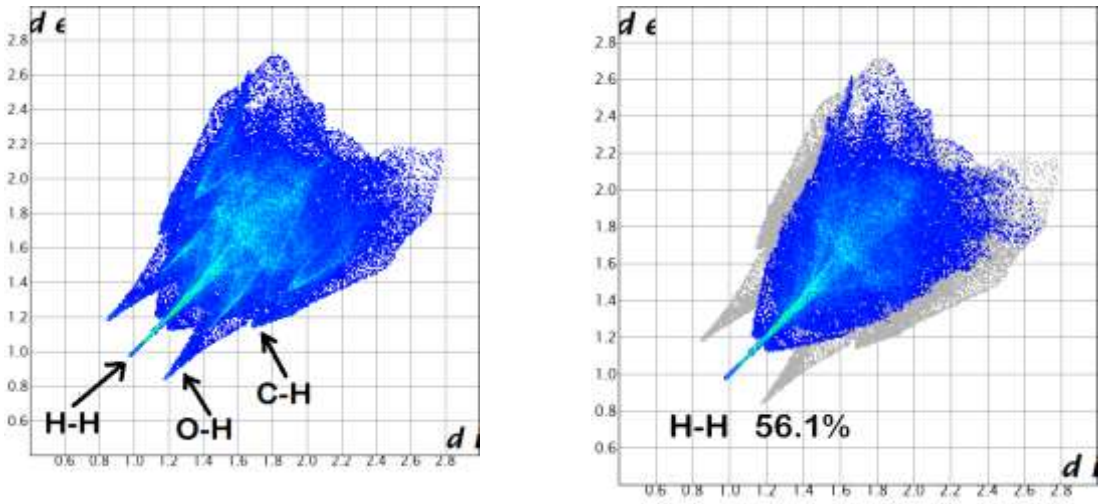

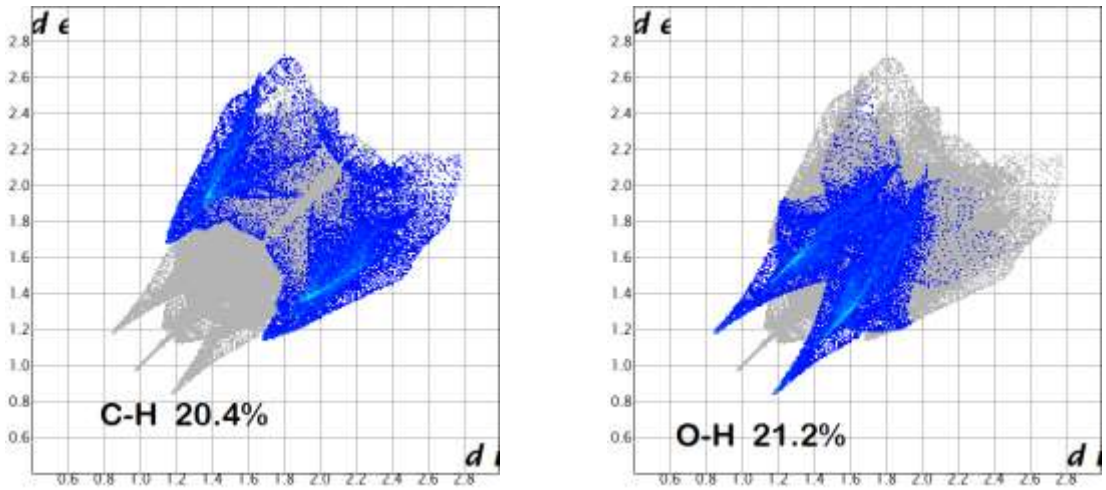

Fig.3(A).12. Finger print plot of **2**: full and resolved into H···H, C···H and O···H contacts showing the percentages of contacts contributed to the total Hirshfeld surface area.

Further, the O···H and C···H FP plots also reveal the information regarding the intermolecular interaction with individual contribution towards crystal packing. O-H interaction (indicated by two sharp symmetric spikes) is one of the most significant contacts in both the complexes. The presence of spikes indicates strong hydrogen bonding interaction [34]. The relative contribution of O···H contacts is found to be 21.2% in complex **2** and 31.1% in complex **1**. It is interesting to note that the FP plot of C-H contacts in complex **2** shows characteristics "wings" which are identified as a result of weak C-H···π interactions. The C-H FP plot in complex **1** does not have any characteristic feature. The red triangles on the shape index represented by concave regions indicate π-stacking interactions whereas the blue triangles represented by convex regions indicate the ring atoms of the molecule inside the surface. The red triangles on the shape index mapping refer to the C-H···π interaction which is in accordance with the 2D FP plot with the contribution of 20.4% in complex **2**. The curvedness indicates the electron density of surface curves around the molecular interactions. The flat areas of the surface correspond to low value of curvedness, while sharp curvature area correspond to high values of curvedness and usually tend to divide the surface into patches, indicating contacts between neighboring molecules. The large flat region delineated by a blue outline refers to π-π stacking interactions. Curvedness of the present compound indicates absence of π-π stacking interactions. All the atom···atom contacts with their relative contribution is summarized in Table 3(A).3. The Hirshfeld surface analysis reveals O-H···O hydrogen bonding, C-H···π interaction and H···H interaction as the primary structural motifs that constitute the molecular crystal. In addition to that C···O, C···N

and C···C interaction in complex **1** while C···O and C···C interaction in complex **2** shows minor contribution to HS of the molecular crystal.

Table 3(A).3 Summary of various contacts and their contributions to the overall HS for compounds 1 and 2.

Type of Contact	Contribution in %	
	I	**2**
H···H	46.0	56.1
C···H	16.4	20.4
O···H	31.1	21.2
N···C	0.9	-
C···C	3.2	0.7
C···O	0.4	1.1

3(A).4.5. Antimicrobial activity study

The ligand and the derived complexes were evaluated for their antimicrobial activity and the data is presented in Table 3(A).4. Negative control plate lacked zone of inhibition while strong inhibition was observed in the presence of chloramphenicol control, which proved the susceptibility of microorganisms to antimicrobial agents.

Ligand did not display any inhibition zone in the range tested. Among the complexes derived Ni(II) complex was found to be inactive, Co(III) complex exhibited antimicrobial activity with MIC of 5mM against *S. aureus* and *B. subtilis*, which are both gram positive bacteria. Also previously, substituted salicylaldehydes have been reported to display antimicrobial activities better than the parent compound salicylaldehyde [35]. We infer from the analysis that cobalt complex possesses antimicrobial activity in contrast to those with Ni(II). The action of Co(III) complex specific to gram positive bacteria can be attributed to the differences in the structure of the bacterial cell wall. Kuzmanović et al. showed the ligand type was the factor determining antimicrobial activity of the cobalt complexes, evaluation of the antimicrobial activity of complexes obtained by switching central metal ions against a single ligand in our work demonstrated that the metal ion is another important parameter that decides antimicrobial activity of the coordination complex[36].

Table 3(A).4. Antimicrobial activity of complexes.

Compound	MIC value in mM			
	E. coli	***P. vulgaris***	***S. aureus***	***B. subtilis***
Ligand (HL2)	>10	>10	>10	>10
$[Co(L2)_2](ClO_4)$	>10	>10	5	5
$[Ni(L2)(HL2)](ClO_4).0.5CH_3OH$	>10	>10	>10	>10
Chloramphenicol	0.0003	0.0015	0.0015	0.003

#MIC in mM

**E. coli* – *Escherichia coli* gram -ve
**P. vulgaris* – *Proteus vulgaris* gram -ve
**S. aureus* – *Staphylococcus aureus* gram + ve
**B. subtilis* – Bacillus subtilis gram +ve

Considering all the mechanistic frameworks currently known for antimicrobial activity of metals [37], it is understood that the antimicrobial activity of Co(III) complex is the result of the ability of cobalt to catalyse the Fention chemistry better than nickel. Overall, the work may contribute to designing metal antimicrobials, which will have applications in all the sectors of life to overcome the global rise of antibiotic resistant micro-organisms.

3(A).5. Conclusions

Two mononuclear octahedral Ni(II) and Co(III) complexes have been synthesized by the reaction between N_2O donor ligand{((2-(phenylamino)ethyl)imino)methyl}phenol (HL2) and metal perchlorate salt in methanol and characterized with structures. Structural data shows two ligands are coordinated to both the metal centres and one ClO_4^- ion outside the coordination sphere. The Hirshfeld surface analysis of complexes **1** and **2** suggest that the molecular crystal structures are stabilized primarily by H···H, C···H and O···H contacts. The short H/H contacts in the crystal structure of complex **2** are arising from the phenyl ring (connected to the single N atom) of the HL2 ligand. Antimicrobial studies demonstrated the antimicrobial potential of the tested Ni(II) and Co(III) complexes against Gram-negative and Gram-positive bacteria. Co(III) complex was found to effectively target Gram-positive bacteria and it is therefore put forward as a promising antimicrobial agent.

3(A).6. References:

1. P. Bhowmik, S. Chattopadhyay, A. Ghosh. Inorg. Chim. Acta 396 (2013) 66.
2. M. Das, S. Chattopadhyay. J. Mol. Struct. 1051 (2013) 250.
3. S. Kathiresan, T. Anand, S. Mugesh, J. Annaraj, J. Photochem. Photobiol. B. Biol 148 (2015) 290.
4. R. S. Joseyphus, C. Shiju, J. Joseph, C. J. Dhanaraj, D. Arish. Spectrochim. Acta Part A: Mol. Biomol. Spectroscopy 133 (2014) 149.
5. S. Basak, S. Sen, S. Mitra, W. S. Sheldrick. Struct. Chem. 19 (2008) 115.
6. M. S. Kasare , P. P. Dhavan, B. L. Jadhav, S. D. Pawar. Chem. Select 4 (2019) 10792.
7. Z. L. You, L. L. Ni, D. H. Shi. Eur. J. Med. Chem. 45 (2010) 3196.
8. M. Hasanzadeh, M. Salehi, M. Kubicki, S. M. Shahcheragh, G. Dutkiewicz, M. Pyziak, A. Khaleghian. Transition Met Chem. 39 (2014) 623.
9. M. Salehi, M. Kubicki, G. Dutkiewicz, A. Rezaei, M. Behzad, S. Etminani. Russ. J. Coord. Chem. 39 (2013) 716.
10. E. Yousif, A. Majeed, K. Al-Sammarrae, N. Salih, J. Salimon, B. Abdullah. Arab. J. Chem. 10 (2017) S1639.
11. J. C. Zhang, X. S. Zhou, X. L. Wang, X. F. Li, Z. L. You. Transition Met. Chem. 36 (2011) 93.
12 M. J. Reimann, D. R. Salmon, J. T. Horton, E. C. Gier, L. R. Jefferies. ACS Omega 4 (2019) 2874.
13 M. Das, S. Chattopadhyay. J. Mol. Struct. 1051 (2013) 250.
14 M. Barwiolek, E. Szlyk, T. M. Muziol, T. Lis. Dalton Trans 40 (2011) 11012.
15 M. Fondo, N. Ocampo, A. M. Garcia-Deibe, I. Garcia-Santos, J. Sanmartin, A. J. Mota, J. L. Perez-Lustres. Dalton Trans 40 (2011) 11770.
16 Z. L. You, M. Zhang, D. M. Xian, H. H. Li, Q. F. Weng. Transition Met Chem. 37 (2012) 279.
17 M. Sakthi, A. Ramu. J. Mol. Struct. 1149 (2017) 727.
18 S. S. Qiana, X. S. Chengb, Z. L. Youb, and H. L. Zhua. Russ. J. Coord. Chem. 39 (2013) 704.
19. Z. Hong. Synth. React. Inorg. Met.Org. Nano-Met. Chem. 40 (2010) 601.
20. F. M. Wang. Synth. React. Inorg. Met Org. Nano-Met. Chem. 43 (2013) 1001.

21. L. W. Xue, Y. J. Han, G. Q. Zhao, Y. X. Feng. Synth. React. Inorg. Met. Org. Nano-Met. Chem. 42 (2012) 154.
22. S. Raje, N. Mondivagu, M. Chahal, R. J. Butcher, R. Angamuthu. Chem. Asian J. 13 (2018) 1458.
23. B. Kumari, S. Kundu, K. Ghosh, M. Banerjee, S. K. Pradhan, S. M. Islam, P. Brandão, V. Félix, D. Das. Dalton Trans 47 (2018) 14008.
24. A. Ghosh, D. Das. Dalton Trans 44 (2015) 11797.
25. H. Peng, Y. L, Zhong, W. Che. Synth. React. Inorg. Met.Org. Nano-Met. Chem. 38 (2008) 677.
26. Agilent, CrysAlis PRO. Agilent Technologies UK Ltd, Yarnton, England, (2011).
27. G.M. Sheldrick, SAINT, 5.1 ed. Siemens Industrial Automation Inc., Madison, WI (1995).
28. G.M. Sheldrick. SHELXL-97: Program for Crystal Structure Refinement, University of Gottingen, Gottingen (1997).
29. K. Nakamoto, Infrared and Raman Spectra of Inorganic and Coordination Compounds. Part B. Applications in Coordination, Organometallic, and Bioinorganic Chemistry, fifth ed., Wiley. New York, (1997) 116.
30 M. J. Turner, J. J. McKinnon, S. K. Wolff, D. J. Grimwood, P. R. Spackman, D. Jayatilaka, M. A. Spackman, CrystalExplorer17. The University of Western Australia (2017).
31 M. A. Spackman, J. Dylan. CrystEngComm. 11 (2009) 19.
32 V.V. Mossine, C. L. Barnes, T. P. Mawhinney. J. Mol. Struct. 1160 (2018) 73.
33. S. L. Tan, M. M. Jotani, E. R. T. Tiekink. Acta Cryst. E75 (2019) 308.
34. H. A. Lamya, J. Jacques, B. Olivier, H. A. Nora, A. E. Ali. Scientific Reports, 9 (2019) 19745.
35. E. Pelttari, M. Lehtinen, H. Elo, Z. Naturforsch. 66c (2011) 571.
36. S. O. Podunavac-Kuzmanovic, V. M. Leova and D. D. Cvetkovi, J. Serb. Chem. Soc. 73 (2008) 1153.
37. J. A. Lemire1, J. J. Harrison, R. J. Turner. Nature Rev. Microbiology 11 (2013) 371.

CHAPTER-3(B)

Mononuclear Ni(II) and Co(III) and trinuclear Cd(II) complexes with N_2O donor Schiff base ligand using substituted salicyldehyde: Syntheses, structures and antimicrobial activity

Abstract

One new N_2O-donor tridentate ligand 2,4-dichloro-6-(((2-(phenylamino)ethyl) imino)methyl)phenol (HL3) has been synthesized and characterized. The tridentate N_2O-coordinate ligand has been used in the synthesis of two mononuclear complexes $[Ni(L3)_2].H_2O$ and $[Co(L3)_2]ClO_4$ and one trinuclear complex $[Cd_3(L3)_4](ClO_4)_2$ and the complexes were characterized by spectroscopic techniques and single crystal X-ray diffraction studies. The molar conductivity data of all the complexes show the Ni(II) complex is non-electrolyte, Co(III) complex is 1:1 electrolyte whereas Cd(II) complex is 1:2 electrolytes. Single crystal X-ray diffraction data shows Ni(II) complex has distorted octahedral geometry and two ligands are coordinated to the nickel centers and one H_2O molecule is outside the coordination sphere but Cd(II) complex is trinuclear where two end Cd centers i.e. Cd(1) and Cd(3) has octahedral geometry and middle cadmium i.e. Cd(2) has distorted tetrahedral geometry. The antimicrobial activity of both the complexes were investigated against Gram positive (*Streptococcus pyogenes*, *Streptococcus aureus*) and Gram negative (*Escherichia Coli*, *Pseudomonas Aeruginosa*) bacteria using Broth Dilution Method. The Ni(II) complex demonstrated significant antimicrobial activity while Co(III) exhibited the best antibacterial activity.

3(B).1. Introduction

Schiff bases have been used as versatile chelating ligand in coordination chemistry as they not only form stable complexes with transition metal ions but also form different geometries due to the presence of different donor atoms. Schiff base ligands with more than two coordination sites are important in this regard [1-10]. In the section A of this chapter, we have reported the reaction of tridentate N_2O-donor Schiff base ligand 2-(((2-(phenylamino)ethyl)imino)methyl)phenol (HL2) with Ni(II) and Co(II) perchlorate salt and formation of mononuclear $[Ni(L2)(HL2)]ClO_4.0.5CH_3OH$ and $[Co(L2)_2]ClO_4$ complexes, respectively [11]. The objective of the research work is to compare the reactivity of another tridentate N_2O donor ligand 2,4-dichloro-6-(((2-(phenylamino)ethyl)imino)methyl)phenol (HL3) with three metal perchlorate salts $M(ClO_4)_2.6H_2O$ [M= Ni(II), Co(II) and Cd(II)].

Here, we report on the synthesis and characterization of two octahedral mononuclear complexes $[Ni(L3)_2].H_2O$ and $[Co(L3)_2]ClO_4$ and one trinuclear Cd(II) complex $[Cd_3(L3)_4](ClO_4)_2$ using the ligand 2,4-dichloro-6-(((2-(phenylamino)ethyl)imino)methyl) phenol (HL3). Antimicrobial activity of Ni(II) and Co(III) complexes are also investigated.

3(B).2. Experimental

3(B).2.1. Materials

The chemicals and solvents were of analytical grade and purchased from commercial sources. 3,5 dichlorosalicyldehyde (Avra), N-phenylethylenediamine (Aldrich) were used as received. $M(ClO_4)_2.6H_2O$ [M = Ni(II), Co(II) and Cd(II)] was prepared by reaction of metal carbonate with dilute $HClO_4$ acid and followed by slow evaporation of the solution over steam bath.

3(B).2.2. Synthesis of Ligand

Synthesis of 2,4-dichloro-6-(((2-(phenylamino)ethyl)imino)methyl)phenol (HL3)

To the solution of N-phenylethene-1,2-diamine (1.361 g, 10 mmol) in ethanol (30 mL), a solution of 3,5-dichlorosalicyldehyde (1.910 g, 10 mmol) in the same solvent (15 mL) was added dropwise with stirring. The reaction mixture was then refluxed for 6 h. The solution was concentrated on a vacuum rotary evaporator and the yellow color solid product was isolated by filtration and recrystallized in hot ethanol.

Yield. 3.00g (92%). Found C = 57.85, H = 4.48, N = 8.90%. Elemental analysis calc. for $C_{15}H_{14}N_2OCl_2$: C = 58.25, H = 4.53, N = 9.06 %. IR (KBr pellet, cm^{-1}): ν(N-H), 3291s; ν(C=N), 1651 s; ν(O-H), 3440. ^{1}H NMR (400 MHz, $CDCl_3$, 20°C δ ppm); 3.54 (t, 2H, N-CH_2 of ethylene), 3.89 (t, 2H, N-CH_2 of ethylene), 6.63-7.41(m, 9H, aromatic protons) 8.22(1H, s, HC=N), 14.39 (1H, s, O-H), λmax/nm (εmax/ mol^{-1} cm^{-1}). 336(64), 250(317), 224(410). MS (ESI): m/z 309.31 $(C_{15}H_{14}Cl_2N_2O)^+$ (100).

3(B).2.3. Syntheses of Complexes

Caution! Transition metal complexes with perchlorate ion and organic ligands are potentially explosive. Complexes should be synthesized in small quantities and handled with care.

3(B).2.3.1. Synthesis of $[Ni(L3)_2].H_2O$ (1)

A solution of ligand HL3 (0.154 g, 0.5 mmol) in methanol was added drop by drop into a solution of nickel perchlorate hexahydrate (0.090g, 0.25mmol) in methanol (10 ml) at room temperature and color changes to light green immediately. The solution was stirred for additional 3 hours, filtered and solution was kept for evaporation at room temperature. Green rectangle shape crystals suitable for single crystal X-ray diffraction were obtained from the mother liquor after several days.

Yield 0.112 g (65%). Found C = 51.65, H = 3.92, N = 7.98%, Elemental analysis calc. for $C_{30}H_{28}N_4O_3Cl_4Ni$: C = 51.97, H = 4.04, N = 8.08 %. IR (KBr pellet)/ cm^{-1}; ν(N-H), 3263m; ν(C=N), 1635s; ν(O-H), 3423. λ_{max}/nm (ε_{max} /mol^{-1} cm^{-1}). 890(61), 576(37), 396(256), 238(1607). μeff = 2.78 BM.

3(B).2.3.2. Synthesis of $[Co(L3)_2]ClO_4$ (2)

The complex was synthesized by using same method as that of complex **1** except cobalt perchlorate hexahydrate was used instead of nickel perchlorate hexahydrate. Dark brown colour solution was stirred for 3 h at room temperature, filtered and filtrate was kept for slow evaporation. Red brown crystalline compound was obtained after two days, filtered and washed with diethyl ether and dried in vacuo.

Yield. 0.135g (69%). Found C = 51.24, H = 3.98, N = 8.04 %. Elemental analysis calc. for $C_{30}H_{26}N_4O_6Cl_5Co$: C = 51.10, H = 3.82, N = 7.94%. ^{1}H NMR (400 MHz, $CDCl_3$, 20°C δ ppm); 3.54 – 3.57 (t, 2H, N-CH_2 of ethylene), 3.86 – 3.89 (t, 2H, N-CH_2 of ethylene), 6.64 -7.44 (m,

9H, aromatic protons) 8.23(1H, s, HC=N). IR (KBr pellet)/ cm^{-1}; ν(N-H) 3221m; ν(C=N), 1644s; ν(ClO_4), 1050s; δ(O-Cl-O), 623s. λ_{max}/nm (ε_{max}/$mol^{-1}cm^{-1}$). 708(13), 396 (259), 326(282), 264(600), 230(831). Λ_M (Ω^{-1} cm^2 mol^{-1}) = 120.

3(B).2.3.3. Synthesis of $[Cd_3(L3)_4](ClO_4)_2$ (3)

The complex was synthesized by using same method as that of complex **1** except cadmium perchlorate hexahydrate was used instead of nickel perchlorate hexahydrate. Light yellow needle shape crystals suitable for single crystal X-ray diffraction were obtained from the mother liquor after several days.

Yield. 0.090 g (61 %). Found C = 40.40, H = 2.60, N = 6.60 %, Elemental analysis calc. for $C_{60}H_{48}N_8O_{12}Cl_{10}Cd_3$: C = 40.80, H = 2.72, N = 6.34 %. IR (KBr pellet)/ cm^{-1}; ν(N-H), 3279m; ν(C=N), 1637s; ν(ClO_4), 1093s; δ(O-Cl-O), 622s. λ_{max}/nm (ε_{max}/$mol^{-1}cm^{-1}$). 397(162), 336(195), 281(294), 246(1590), 226 (1886). Λ_M (Ω^{-1} cm^2 mol^{-1}) = 230.

3(B).2.4. Physical Measurements

The IR spectra were recorded on Bruker alpha FT-IR spectrometer using KBr pellet. UV-Vis spectra (850 - 190 nm) of the ligand and complexes were recorded on a JASCO V630 in CH_3CN solution (1 x 10^{-3} M). ^1H NMR spectra were recorded on Bruker NMR AV400. The elemental analysis (C, H and N) were carried out using a Thermo Finnigan FLASH EA 1112 series elemental analyzer. Solution conductivity were measured in acetonitrile solution using Equip-Tronics conductivity meter (model no. EQ660 A). Room temperature magnetic susceptibilities of powder samples were measured using Guoy balance.

3(B).2.5. Antimicrobial activity assay

The compounds were screened for antimicrobial activity using broth dilution method where the growth of microorganism was checked in the presence of the test compounds. For this, the standard strains from MTCC viz., Gram positive (*Streptococcus pyogenes*, *Streptococcus aureus*) and Gram negative (*Escherichia Coli*, *Pseudomonas Aeruginosa*) were used. The test compounds were dissolved in DMSO and diluted with Muller-Hinton broth media in desired concentrations. The test was performed in test tubes. The tubes were inoculated with the test organisms. The tubes without any drug or compound treatment were kept as negative controls. Test compounds were added to the sample test tubes. Gentamicin 0.05 to 0.5

mM was used as a reference compound. All the tubes were incubated at 37°C overnight. The growth of the organisms in the test or reference tubes was checked and compared with that of the negative control tubes. Minimal inhibitory concentration (MIC) was defined as the lowest concentration of the test compound that inhibited the visible growth of the microorganism.

3(B).3. X-ray Crystallography

The X-ray single crystal data of the Ni(II) and Cd(II) complexes were collected on an Xtlab Synergy Rigaku oxford diffraction with HyPix – 3000 detector, equipped with graphite monochromated Mo Kα radiation (λ = 0.71073 Å) at 293K. The 2θ range for data collection were from 5.082 to 50^0 for Ni(II) and 4 to 53.86^0 for Cd(II) complexes. The data interpretations were processed with CrysAlisPro, Xtlab Synergy Rigaku oxford diffraction Version 171.39 [12,13]. Absorption corrections were applied based on multi-scan method [14]. The structures were solved by direct methods and refined by the full-matrix least-square method based on F^2 technique using SHELXL-97 program package [15]. All calculations were carried out using WinGX system Ver-1.64 crystallographic software [16]. All non-hydrogen atoms were refined anisotropically. The positions of the hydrogen atoms were added to their geometrically ideal position. ORTEP3 for Windows program were used for generating for molecular graphics [17].

3(B).4. Results and discussion

3(B).4.1. Synthesis of the ligand (HL3) and complexes

The Schiff base ligand (HL3) was synthesized as a yellow solid by the condensation of 3,5-dichlorosalicyldehyde and N-Phenylethylenediamine in ethanol [Scheme 3(B).1]. The ligand was characterized by ^{1}H NMR, IR and UV-visible spectral data. The ligand is tridentate with N_2O- coordination sites.

Mononuclear octahedral Ni(II) and Co(III) and trinuclear Cd(II) complexes have been synthesized with good yield (>60%) upon one-pot synthesis of 1:2 molar ratio of metal perchlorate hexahydrate and tridentate Schiff base HL3 in methanol at room temperature [Scheme 3(B).2]. Molar conductivity measurements in CH_3CN shows Ni(II) complex is non-electrolyte but Co(III) complex is 1:1 electrolyte and Cd(II) complexes is 1:2 electrolyte indicating the presence of ClO_4^- ion outside the coordination spheres of Co(III) and Cd(II)

Table 3(B).1 Crystallographic parameters of the complexes 1 and 3.

	$[Ni(L3)_2].H_2O$	**$[Cd_3(L3)_4](ClO_4)_2$**
Empirical formula	$C_{30}H_{28}Cl_4N_4NiO_3$	$C_{30}H_{24}Cd_{1.5}Cl_5N_4O_{6.5}$
Formula weight	693.07	890.428
Temperature/K	293(2)	302.3(5)
Crystal system	Triclinic	Monoclinic
Space group	*P-1*	*P2/c*
a/Å	8.1597(4)	13.6541(9)
b/Å	13.7443(5)	16.5562(4)
c/Å	14.6233(7)	25.0204(17)
α/°	112.801(4)	90
β/°	99.918(4)	139.891(14)
γ/°	90.164(3)	90
Volume/$Å^3$	1484.86(12)	3643.9(11)
Z	2	4
ρ_{calc} g/cm^3	1.550	1.623
μ/mm^{-1}	1.053	1.296
F(000)	712.0	1763.1
Crystal size/mm^3	0.2 × 0.15 × 0.1	0.3 × 0.2 × 0.2
Radiation	Mo Kα (λ = 0.71073)	Mo Kα (λ = 0.71073)
2θ range for data collection/°	5.082 to 50	4 to 53.86
Index ranges	$-9 \le h \le 9$, $-16 \le k \le 16$, $-17 \le l \le 17$	$-17 \le h \le 17$, $-20 \le k \le 21$, $-31 \le l \le 30$
Reflections collected	29781	43765
Independent reflections	5142 [R_{int} = 0.1596, R_{sigma} = 0.0803]	7629 [R_{int} = 0.0493, R_{sigma} = 0.0397]
Data/restraints/parameters	5142/9/385	7629/0/403
Goodness-of-fit on F^2	1.235	1.038
Final R indexes [I>=2σ (I)]	R_1 = 0.0810, wR_2 = 0.2095	R_1 = 0.0474, wR_2 = 0.1458

Final R indexes [all data]	R_1 = 0.1030, wR_2 = 0.2267	R_1 = 0.0667, wR_2 = 0.1612
Largest diff. peak/hole/e $Å^{-3}$	1.33/-1.05	1.50/-0.65
CCDC number	2160855	2167122

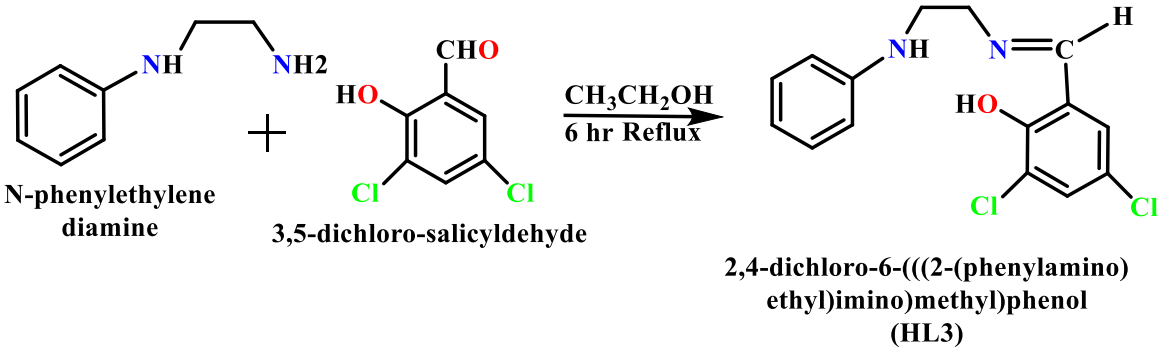

,

Scheme 3(B). 1. Synthesis of the ligand (HL3)

complexes. The molecular composition of the complexes was confirmed by elemental analyses and single crystal X-ray diffraction studies. Both Ni(II) and Co(III) complexes are mononuclear with two L3 ligands in the coordination sphere and they have octahedral geometry. In the Co(III) complex, two ligands are coordinated and one ClO_4^- ion outside the coordination sphere in order to balance the charge. The Cd(II) complex is trinuclear and Cd1 and Cd3 centers have octahedral geometry and Cd2 center has distorted tetrahedral geometry. We are unable to obtain single crystal of Co(III) complex even after several attempts. The compounds are soluble in all common organic solvents like acetonitrile, methanol, ethanol, acetone, dichloromethane etc.

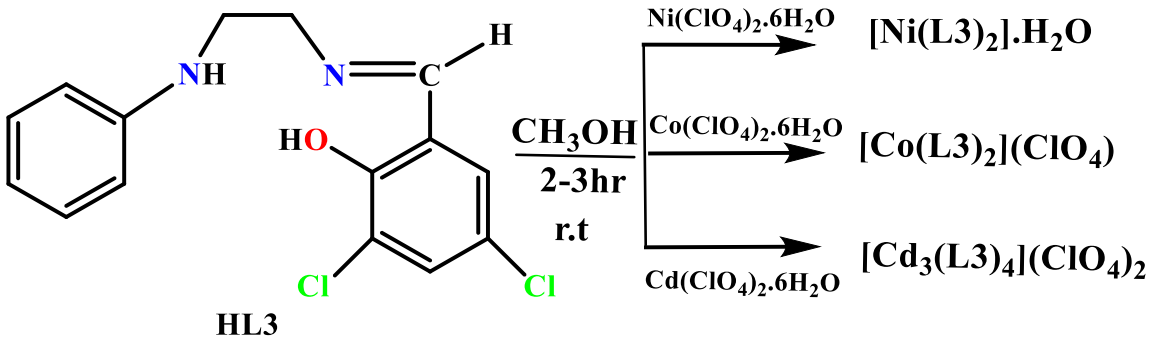

Scheme 3(B).2. Syntheses of the complexes

3(B).4.2. Spectral Data

3(B).4.2.1. ^{1}H NMR and Mass spectral data

The ^{1}H NMR spectra of ligand (HL3) shows two triplets appeared in the region at 3.54 – 3.89 ppm confirming the presence of –CH_2–CH_2– group of ethylenediamine moiety. One singlet appear at 14.39 ppm confirms the presence of OH group and another singlet appeared at 8.22 ppm confirming the presence of imine(HC=N) group. The aromatic protons of phenyl ring appeared at 6.63-7.41 ppm as multiplet.

The ^{1}H NMR data for the cobalt(III) complex recorded in $CDCl_3$. All the aromatic protons and imine proton of the coordinated Schiff base ligand appear in the region of 6.64 – 7.44 ppm and protons appeared in the region of 3.54 to 3.89 ppm are assigned to N-CH_2-CH_2-N protons.

Mass spectra of the synthesized Schiff base ligand (HL3) confirmed the proposed formula by detecting the following peaks. The observed peak at m/z 308.3 $(C_{15}H_{13}N_2OCl_2)^+$, represents the molecular ion peak of the Schiff base with 100% abundance. The other molecular ion peaks m/z 106 and 203 appeared in the spectra are attributed to the fragmentation of molecule obtained from the rupture of different bonds present the molecule. The Mass Spectra of Co(III) complex showed molecular ion peaks at m/z 677 corresponds to $[Co(C_{15}H_{13}N_2OCl_2)_2]^+$

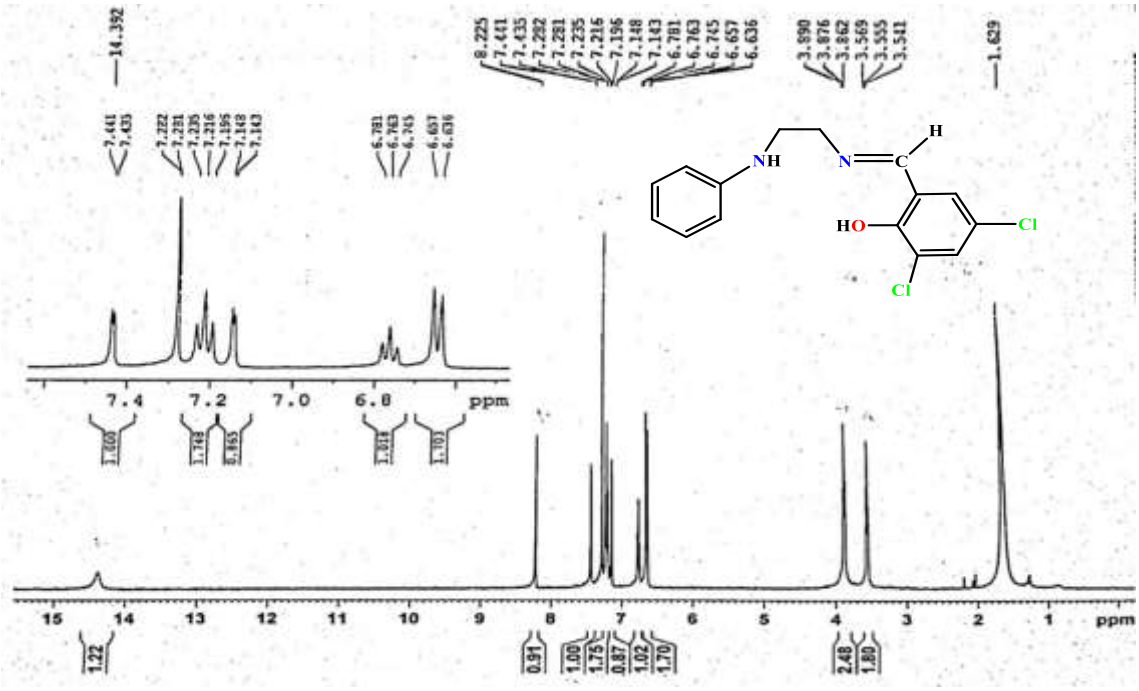

Figure. 3(B). 1. ^{1}H NMR spectrum of Ligand (HL3)

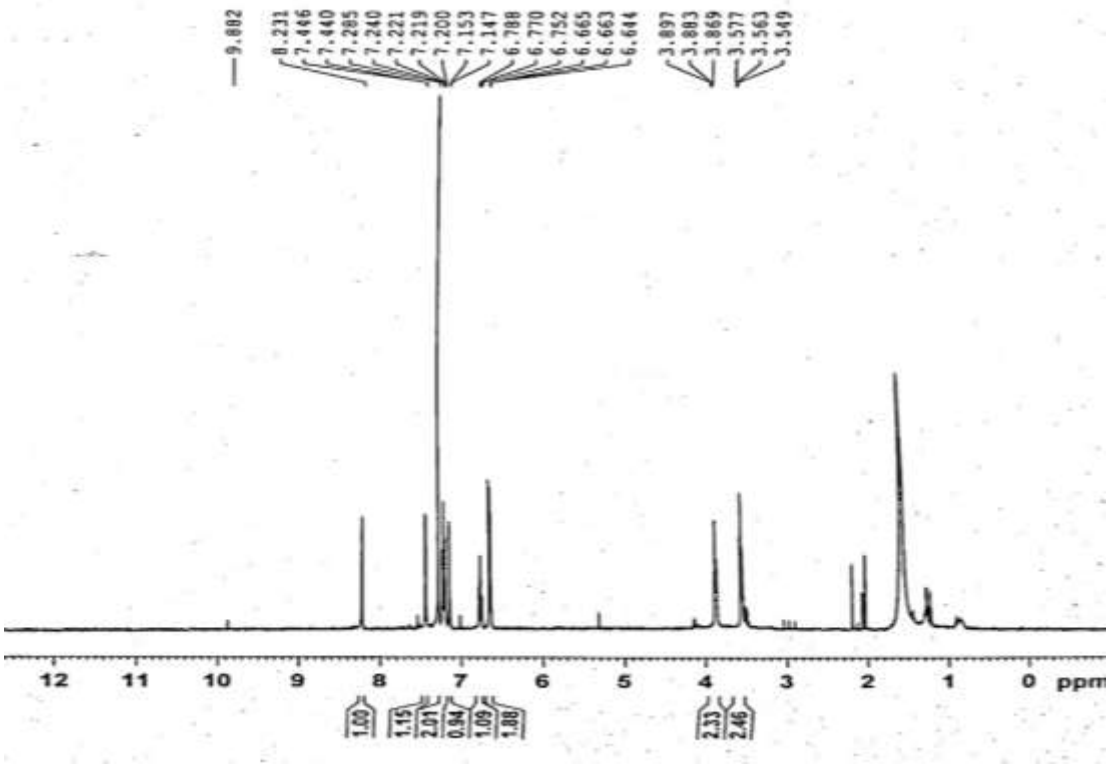

Figure. 3(B). 2. ^{1}H NMR Spectrum of $[Co(L3)_2]ClO_4$

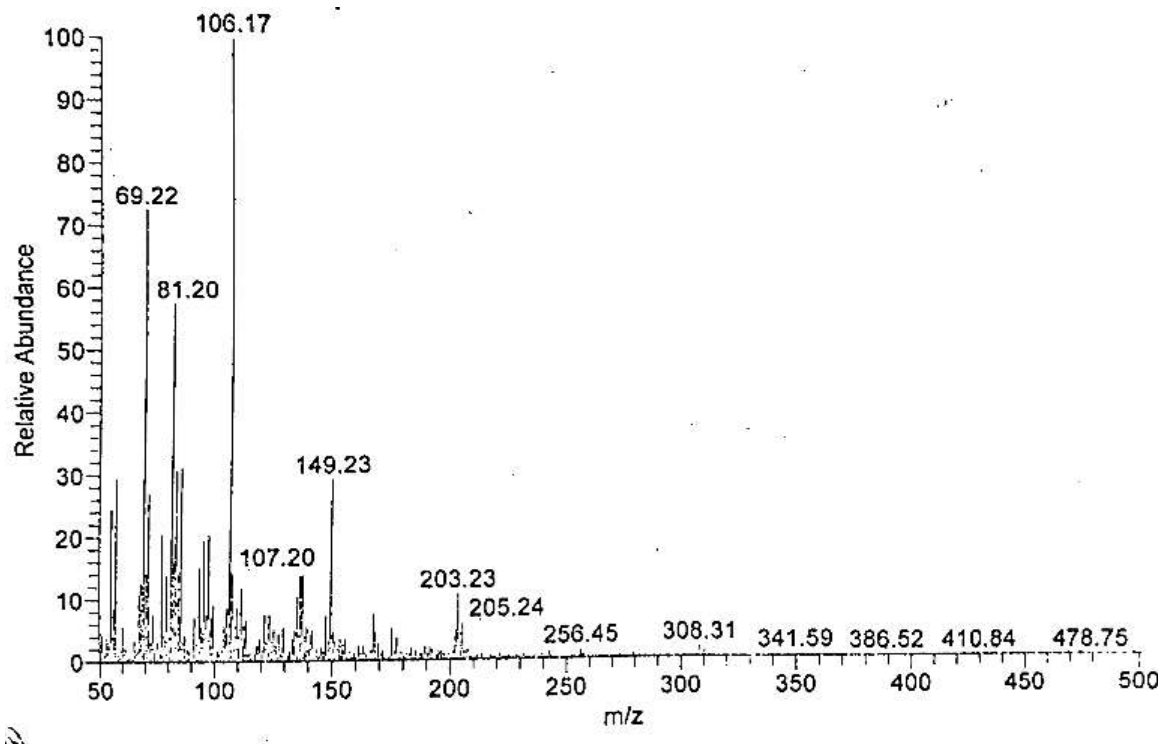

Figure. 3(B). 3. Mass spectrum of Ligand(HL3)

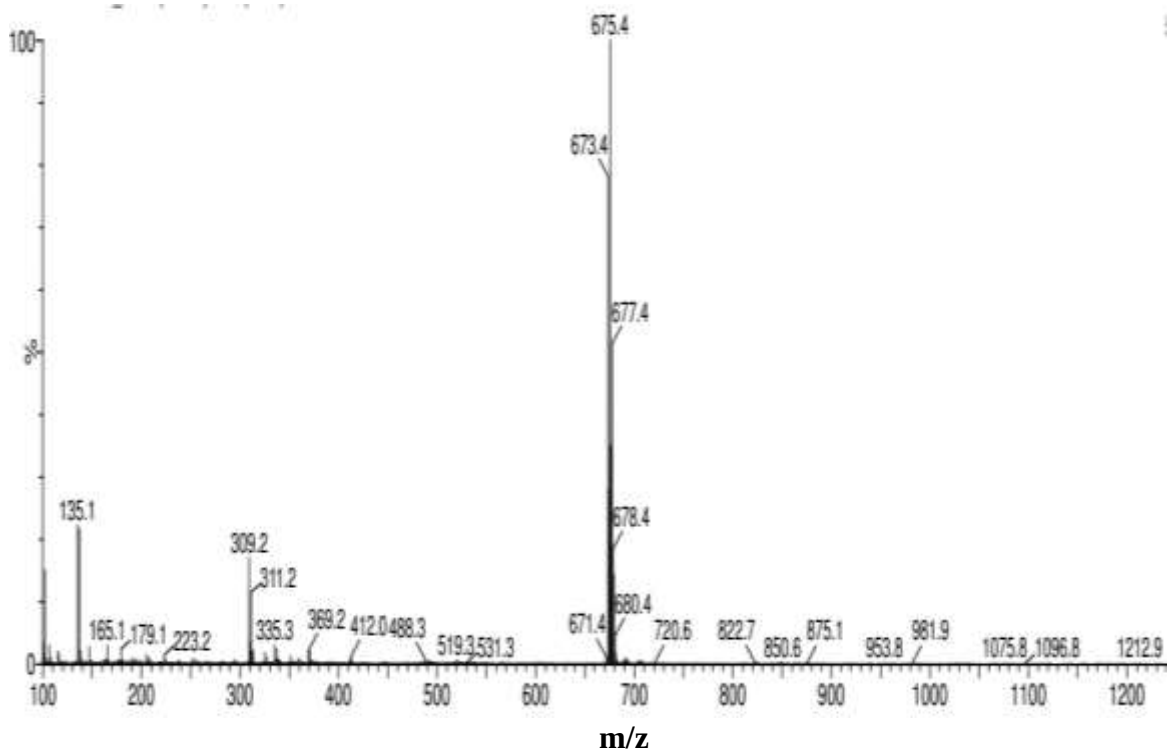

Figure. 3(B). 4. ESI-Mass spectrum of $[Co(L3)_2]ClO_4$

3(B).4.2.3. IR spectral data

IR-spectrum of ligand exhibits several strong bands. Among these, one strong band occurred at 3291 cm^{-1} due to ν(N-H), one sharp band at 1651 cm^{-1} due to ν(C=N) and one broad band at 3440 cm^{-1} due to ν(O-H).

The IR spectra of the complexes were assigned with respect to IR spectra of the free ligand HL3 in order to determine the coordination of ligand the metal centers. One strong absorption bands exhibited at ~1600 $cm^{-1}$of the complexes as well as ligand and the bands are shifted to lower wave numbers in the range of 5-10 cm^{-1} in the complexes in comparison to ligand which may be attributed to the coordination of the imine nitrogen atom to the metal centers in the complexes. One weak and broad absorption band ~3423 cm^{-1} for complex **1** is due to ν(O-H) vibration of the H_2O molecule. One weak but sharp band appeared at ~3263 cm^{-1} due to ν(N-H) group for all the complexes. Co(III) and Cd(II) complexes exhibited a broad absorption band at ~1050 cm^{-1} due to ν(ClO_4^-) and a weak band at ~623cm^{-1} due to δ(O-Cl-O) indicating non-coordinating ClO_4^- outside the coordination sphere [18].

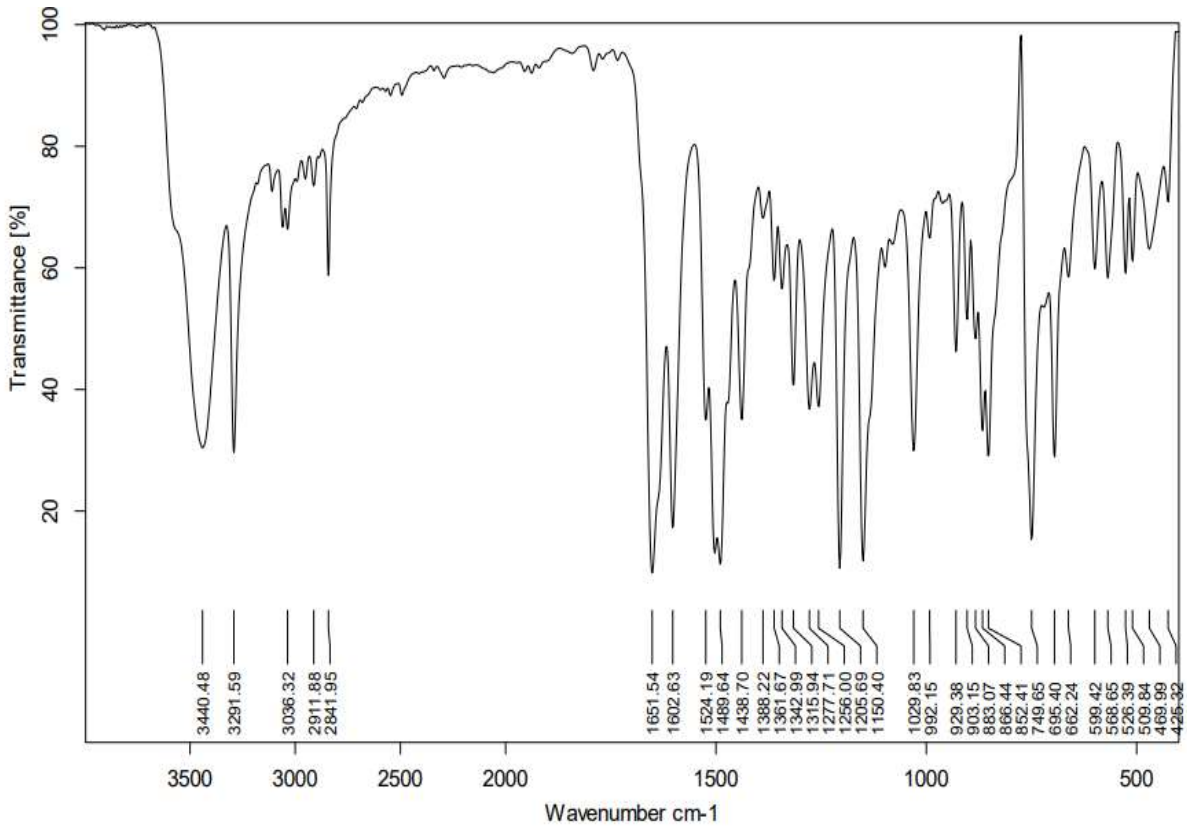

Figure. 3(B). 5. IR spectrum of Ligand (HL3)

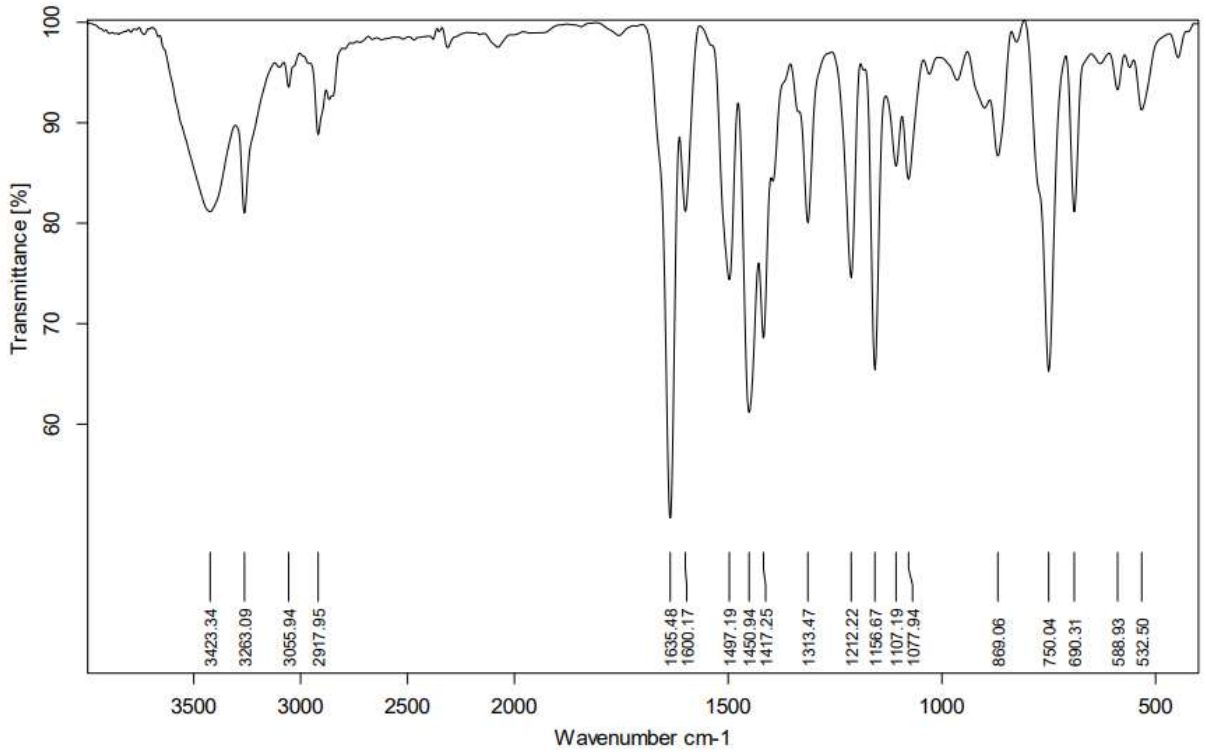

Figure. 3(B). 6. IR spectrum of $[Ni(L)_2].H2O$

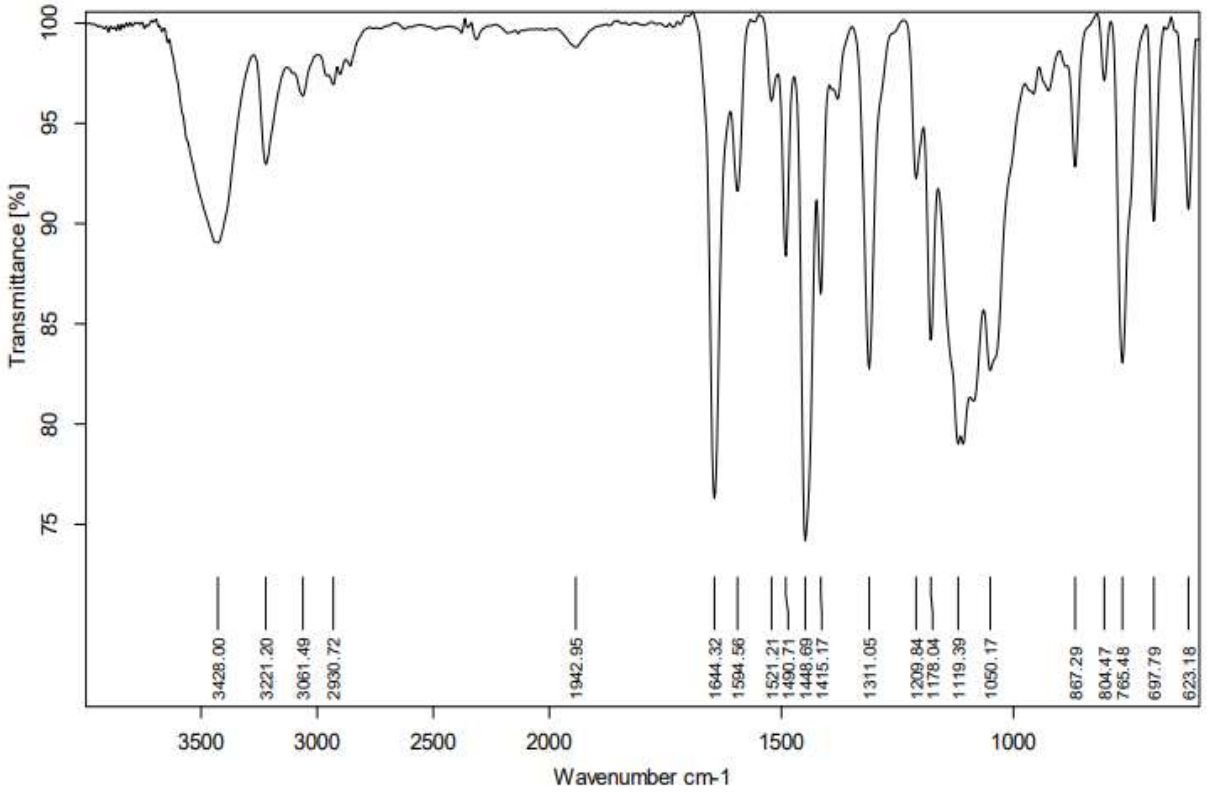

Figure. 3(B). 7. IR spectrum of $[Co(L3)_2]ClO_4$

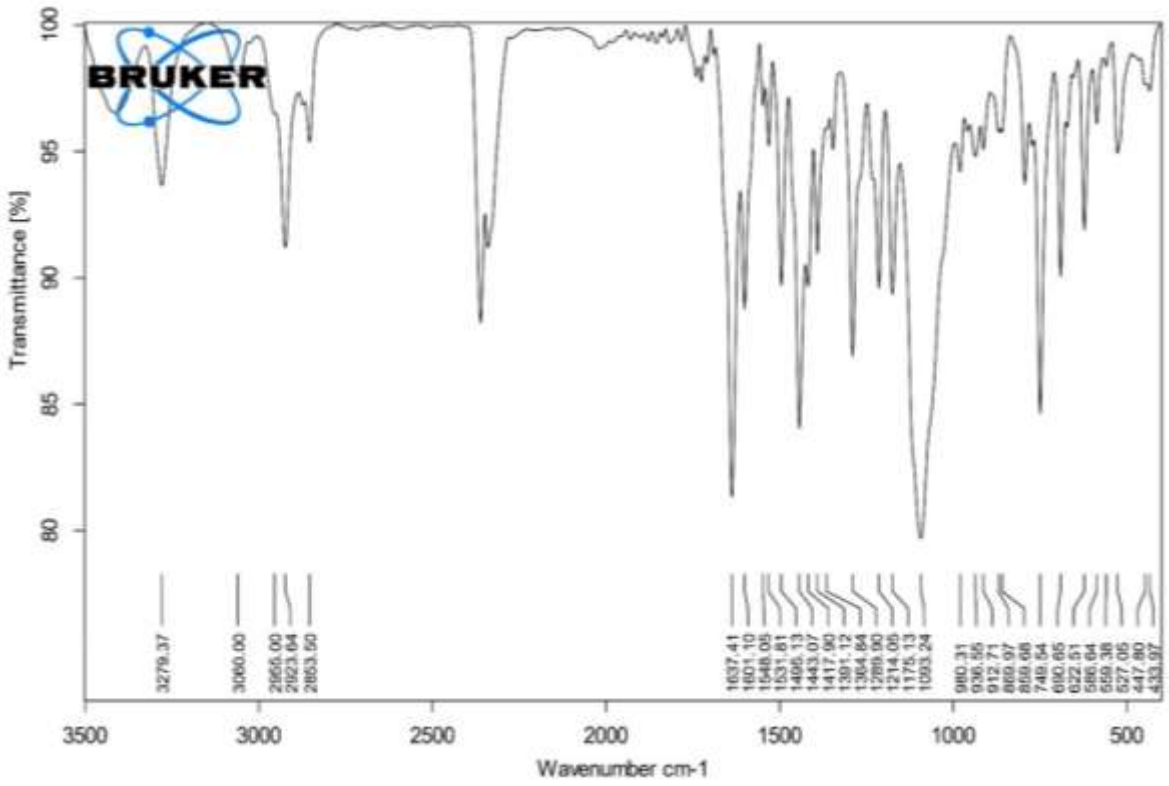

Figure. 3(B). 8. IR spectrum of $[Cd_3(L3)_4](ClO_4)_2$

3(B).4.2.4. Electronic Spectra

The electronic spectra of all the complexes were drawn in CH_3CN solution at room temperature. The higher energy bands observed at less than 400 nm are due to intra ligand charge transfer transition .The nickel(II) complex exhibited two absorption bands at 890 nm and 576 nm with molar extinction coefficient 61 and 37 L mol^{-1} cm^{-1}, respectively and these are due to d-d transition. The cobalt(II) complex shows one absorption band at 708 nm with molar extinction coefficient 13 L mol^{-1} cm^{-1} due to d-d transition [19].

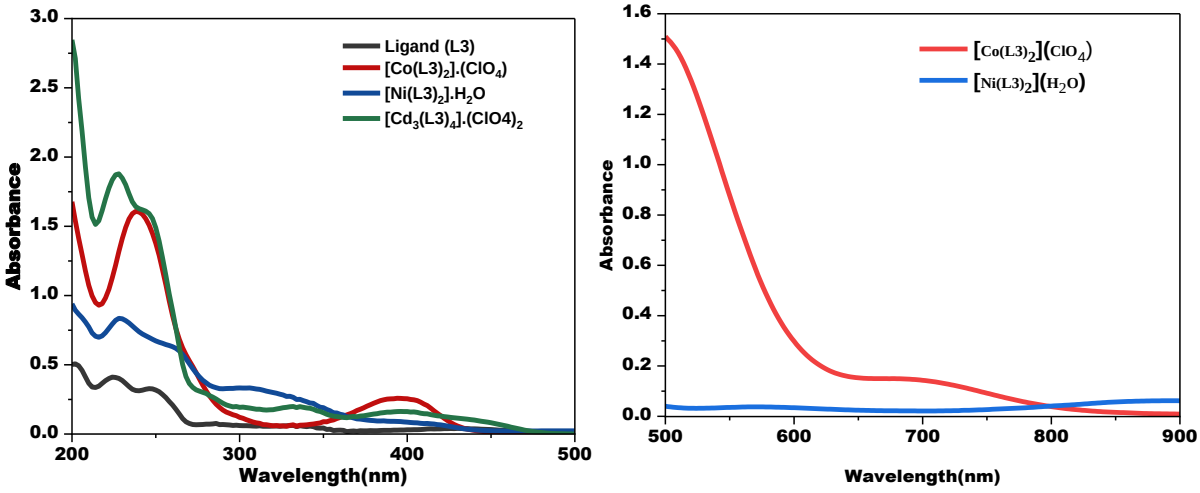

Figure. 3(B). 9. Electronic spectra of the complexes in CH_3CN (10^{-3} M)

3(B).4.2.5. Magnetic studies

The magnetic susceptibility measurement of the powder samples show the effective magnetic moment (μ_{eff}) of the Ni(II) complex at room temperature is 2.80 B.M., indicating two electrons paramagnetic but cobalt complex is diamagnetic indicating it has +3 oxidation state.

3(B).4.3. Description of crystal structures

3(B).4.3.1. Crystal of structure of $[Ni(L3)_2].H_2O$

The ORTEP diagram of the complex with atom-labeling scheme is shown in Fig. 3(B).10(a) and selected bond lengths and angles are given in Table 3(B).2. The molecule crystallizes in triclinic crystal system with space group *P-1*. The structure determination confirmed that the complex **1** is nonionic and one water molecule is present outside the coordination sphere. In the structure, nickel(II) has six coordination using four nitrogen atoms N1, N2, N3, N4 and two oxygen atoms O1, O2 from two tridentate N_2O donor ligands. The equatorial positions of the octahedron are occupied by three nitrogen atoms N1, N2, N6 and oxygen atom O2 and the axial positions are occupied by one nitrogen atom N4 and one oxygen atom O1. The bond distance Ni–N1(2.292 Å) is longer than the other three bonds Ni–N2(1.997 Å), Ni–N6(1.998 Å) and Ni–2(2.042 Å) in the equatorial plane. The two axial bond distances Ni–N4(2.304 Å) and Ni–O1(2.035 Å) are not equal and the axial bond angle N4-Ni-O1 (171.21) is not linear. The geometry around the nickel (II) center is distorted octahedral which can be described from unequal bond angle and bond lengths.

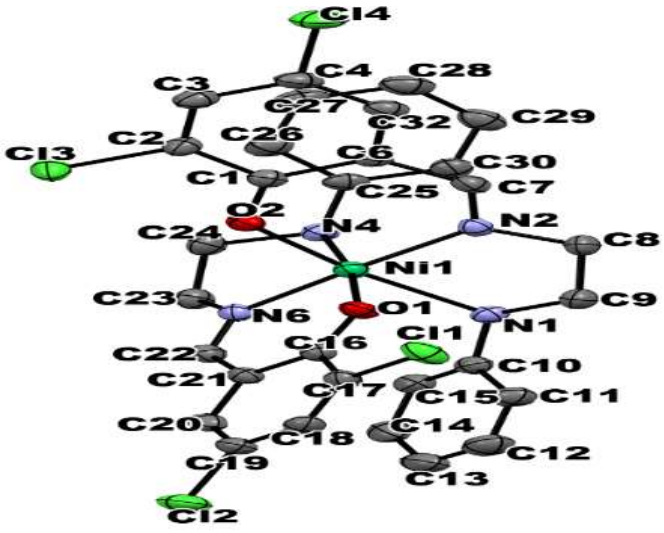

(a)

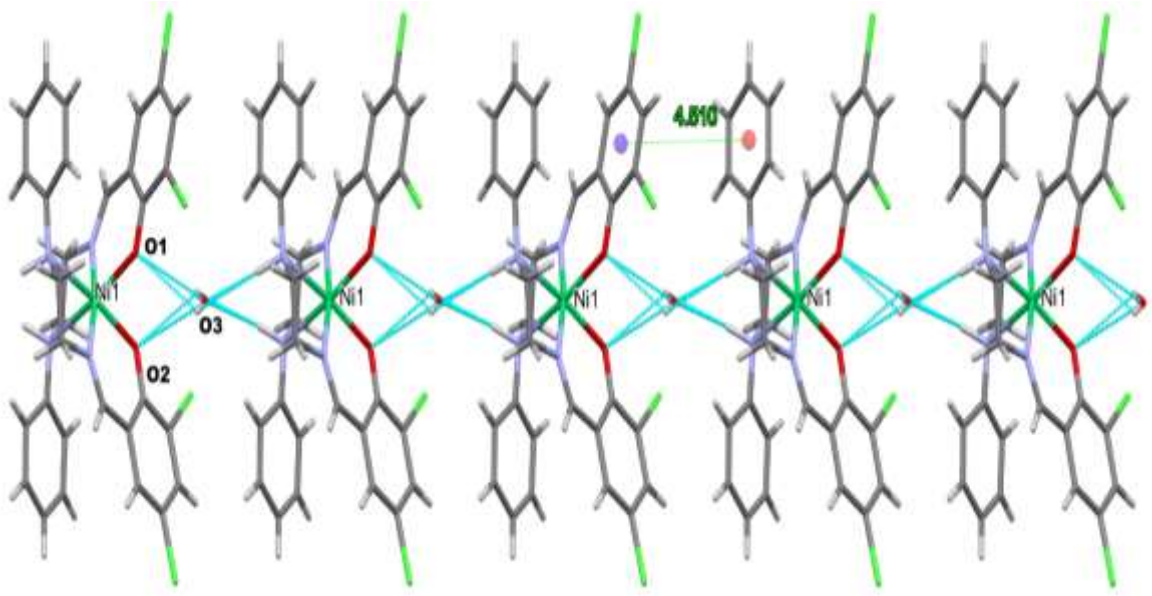

(b)

Figure. 3(B).10 (a). ORTEP diagram of the Ni(II) complex with atom numbering scheme. Hydrogen atoms and H_2O are omitted for clarity. (b). Short intermolecular interactions in the complex.

The O3 of water molecule has two short intermolecular interactions with H of N-H of two nearest ligands in the complex and both O1 and O2 of the ligand have hydrogen bonding with H-O3 of water molecule [Fig. 3(B).10(b)].

3(B).4.3.2. Crystal structure of $[Cd_3(L3)_4](ClO_4)$

The ORTEP diagram of the cationic part of the complex with atom-labeling scheme is shown in Fig. 3(b).11 and selected bond lengths and angles are given in Table 3(B).2. The molecule crystallizes in monoclinic crystal system with space group P2/c. The structure data confirmed that the complex **3** is triatomic and two Cd centers i.e. Cd1 and Cd3 have octahedral geometry whereas Cd2 has distorted tetrahedral geometry. In the structure, Cd1 and Cd2 has six coordination using four nitrogen atoms and two oxygen atoms from two tridentate N2O donor ligands. The equatorial positions of the octahedron are occupied by two imine nitrogen atoms N1 and N4 and two oxygen atoms from two N_2O donor ligand and the axial positions are occupied by two tertiary nitrogen atoms N2 and N3 from two ligands. The bond distances of Cd1–N1, Cd1-N1′ and Cd3–N4, Cd3-N4′ are nearly same (~2.287(4)Å). Similarly, the bond distances of Cd1–N2, Cd1-N2′ and Cd3–N3, Cd3-N3′ are same (2.450 Å) but little longer than

Cd-N1and Cd-N4 bond distances. In Cd2, the four tetrahedral bonds are due to four bridging oxygen atoms from four coordinated N_2O donor ligands of the two Cd centers (Cd1 and Cd3)and all the four Cd2-O bonds are almost same (~2.178Å) but the angles of O-Cd-O are different from ideal tetrahedral angles. The structure shows 4 Cd-Cl interactions which are very weak as the distances are quite high (3.089Å). The geometry around the Cd1 and Cd2(II) centers is distorted octahedral and Cd3 center is distorted tetrahedral which can be described from unequal bond angles.

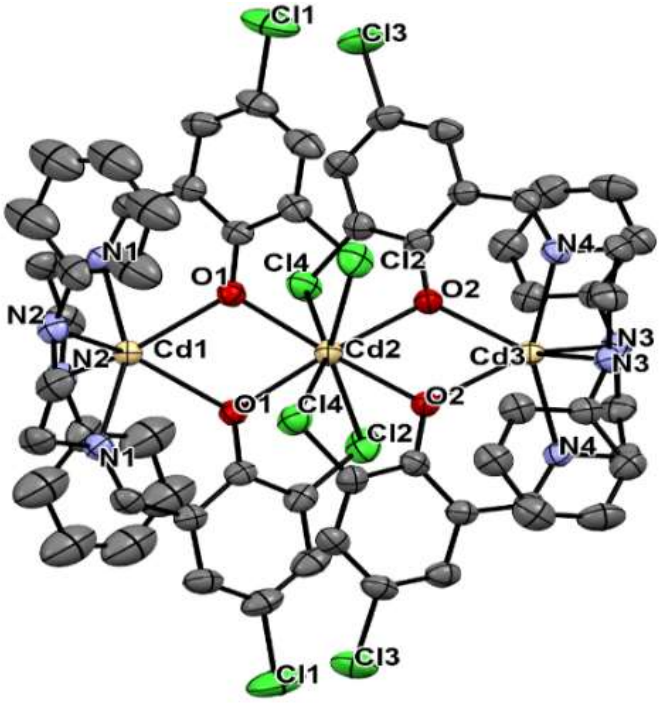

Figure. 3(B).11. Structure of the cationic part of Cd(II) complex with atom numbering scheme. Hydrogen atom and perchlorate molecules are omitted for clarity.

Table 3(B).2 Bond lengths (Å) and bond angles (^{0}) of the complexes.

Bond lengths (Å)				Bond angles (^{0})			
$[Ni(L3)_2].H_2O$		$[Cd_3(L3)_4](ClO_4)_2$		$[Ni(L3)_2].H_2O$		$[Cd_3(L3)_4](ClO_4)_2$	
Ni1-O2	2.042(4)	Cd1-O1	2.295(3)	O2-Ni1-N4	88.84(16)	$O1^1$-Cd1-O1	74.40(15)
Ni1-N2	1.997(4)	Cd1-N1	2.287(4)	O2-Ni1-N1	170.97(13)	N1-Cd1-O1	78.06(13)
Ni1-O1	2.035(4)	Cd1-N2	2.452(4)	N2-Ni1-O2	90.44(16)	$N1^1$-Cd1-O1	122.57(13)
Ni1-N6	1.998(4)	Cd3-O2	2.278(3)	N2-Ni1-O1	95.22(15)	N1-Cd1-$N1^1$	156.0(2)
Ni1-N4	2.304(4)	Cd3-N4	2.288(4)	N2-Ni1-N6	171.48(19)	$N2^1$-Cd1-$O1^1$	136.66(13)
Ni1-N1	2.292(4)	Cd3-N3	2.450(4)	N2-Ni1-N4	93.56(16)	N4-Cd3-$O2^1$	121.34(13)
		Cd2-O1	2.178(3)	N2-Ni1-N1	80.55(16)	$N4^1$-Cd3-$O2^1$	78.97(13)
		Cd2-O2	2.205(3)	O1-Ni1-O2	91.64(15)	N4-Cd3-$N4^1$	156.09(19)
				O1-Ni1-N4	171.21(14)	$N3^1$-Cd3-$O2^1$	142.84(13)
				O1-Ni1-N1	88.61(16)	$N3^1$-Cd3-O2	97.93(12)
				N6-Ni1-O2	95.40(15)	O1-Cd2-O2	142.03(11)

3(B).4.4. Antimicrobial activity study

The synthesized nickel(II) and cobalt(III) complexes were screened for antibacterial activity against Gram positive (*Streptococcus pyogenes*, *Streptococcus aureus*) and Gram negative (*Escherichia Coli*, *Pseudomonas Aeruginosa*) bacteria using Broth Dilution Method.

The MIC (minimum inhibitory concentration) values of the complexes are summarized in the Table 3(b).3. The cobalt (III) complex show considerable activity whereas nickel (II) complex show moderate activity against bacterial strain tested. The result indicates that at 4mM concentration, nickel (II) complex is active against *S. Pyogenes*(Gram negative) bacteria. Cobalt (III) complex is more active against *P. aeruginosa (*Gram Positive) and *S. Pyogenes* (Gram negative) bacteria at the concentration of 2.5 mM and 2 mM respectively. Both the complexes are active against *S. Pyogenes* bacteria. Ni(II) is less effective against Gram negative than HL3 but more effective than HL3 against Gram positive bacteria. Antibacterial activity improved significantly upon complexation as is suggested by the MIC values of cobalt complex against both Gram positive and Gram negative bacteria and Ni complex against gram positive bacteria [20-23].

Table 3(B).3 Antimicrobial activity of the Schiff base ligand and complexes.

Compound	**MIC value in mM**			
	E. Coli	***P. aeruginosa***	***S. aureus***	***S. Pyogenes***
HL3	5	5	10	5
$[Co((L3)_2]ClO_4$	5	2.5	4	2
$[Ni(L3)]_2.H_2O$	10	10	5	4
Gentamycin	0.002	0.004	0.001	0.002

#MIC in mM

*E. coli – *Escherichia coli* gram -ve

*P. aeruginosa – *Pseudomonas Aeruginosa* -ve

*S. aureus – *Staphylococcus aureus* gram +ve

*S. pyogenes – *Streptococcus pyogenes* gram +ve.

3(B).5. Conclusion

One new N_2O-donor tridentate ligand 2,4-dichloro-6-(((2-(phenylamino)ethyl)imino)methyl) phenol (HL3), two mononuclear complexes $[Ni(L3)_2].H_2O$ and $[Co(L3)_2]ClO_4$ and one trinuclear complex $[Cd_3(L3)_4](ClO_4)_2$ have been synthesized and characterized. Single crystal X-ray diffraction data shows Ni(II) complex has distorted octahedral geometry and two ligands are coordinated to the metal centers and one H_2O ion outside the coordination sphere whereas Cd(II) complex is trinuclear and Cd(1) and Cd(3) has octahedral geometry but Cd(2) has distorted tetrahedral geometry. Antibacterial activity has improved significantly upon complexation as is suggested by the MIC values of cobalt(III) complex against both Gram positive and Gram-negative bacteria and nickel(II) complex against Gram positive bacteria.

3(B).6. References

1 N. Ozbek, G. Kavak, Y.Ozcan, S. Ide, N. Karacan. J. Mol. Struct. 919 (2009) 154.

2 L. L. de Oliveira, S.M. da Silva, A. C. A. Casagrande, R. Stieler, O. L. Casagrande. J. Appl. Organomet. Chem. (2018) 4414.

3 S. Raje, S. Gurusamy, A. Koner, S. Mehrotra, S. J. Jennifer, P. G. Vasudev, Ray J. Butcher, R. Angamuthu. Chem. Asian J. 11 (2016) 128.

4 S. Kumar, S. K. Mittal, N. Kaur. Anal. Methods 11 (2019) 359.

5 S. Thakur, M. G. B. Drew, A. Franconetti, A. Frontera, S. Chattopadhyay. RSC Adv. 9 (2019) 4789.

6 S. Sangeeta, K. Ahmad, N. Noorussabah, S. Bharti, M. K. Mishra, S. R. Sharma, M. Choudhary. J. Mol. Struct. 1156 (2018) 1.

7 A. A. Alothman, E. S. Al-Farraj, W. A. Al-Onazi, Z. M. Almarhoon, A. M. Al-Mohaimeed. Arabian Journal of Chemistry 13 (2020) 3889.

8 N. Dave, H. Bhatt. Asian J. Chem. Sci. 98 (2021) 107.

9 R. Jayarajan, G. Vasuki, P. S. Rao. Org. Chem. Int. (2010) 648589.

10 M. Pervaiz, S. Sadiq, A. Sadiq, U. Younas, A. Ashraf, Z. Saeed, M. Zuber, A. Adnan. Coord. Chem. Rev. 447 (2021) 214128.

11 S. J. Munshi, M. Guin, S. Kundu, S. B. Kumar. J. Ind. Chem. Soc. 98 (2021) 10008.

12 Rigaku OD Crys Alis PRO. Rigaku Oxford Differaction Ltd, Yarnton, England (2018).

13 Agilent, CrysAlis PRO. Agilent Technologies UK Ltd, Yarnton, England (2011).

14 G. M. Sheldrick. SAINT, 5.1st edn. Siemens Industrial Automation Inc., Madison, WI (1995).

15 G. M. Sheldrick, Program for Refinement of Crystal Structures, University of Göttingen, Germany (1997).

16 L. J. Farrugia. J. Appl Cryst. 32 (1999) 837.

17 L. J. Farrugia. J. Appl. Cryst. 30 (1997) 565.

18 K. Nakamoto. Infrared and Raman spectra of Inorganic and Coordination Compounds, Part B. Applications in Coordination, Organometallic, and Bioinorganic Chemistry, fifth ed., Wiley, New York (1997) 116.

19 M. Salehi, M. Kubicki, G. Dutkiewicz, A. Rezaei, M. Behzad, S. Etminani. Russ. J. Coord. Chem. 39 (2013) 716.

20 E. Ispir, S. Toroglu, A. Kayraldiz. Transition Met. Chem. 33 (2008) 953.

21 V. P. Radha, S. Chitra, S. Jonekirubavathi, I. Chung, S. Kim, M. Prabakaran. J. Coord. Chem. 73 (2020) 1009.

22 K. B. Gudasi, M.S. Patil, R.S. Vadavi, R.V. Shenoy, S.A. Patil, M. Nethaji. Transition Met. Chem. 31 (2006) 580.

23 S. Chandra, D. Jain, A.K. Sharma, P. Sharma. Molecules 14 (2009) 174.